

Evaluation of Erosion Wear of Turbine Steels in Hydropower Plants

A Dissertation Submitted
In Partial Fulfillment of the Requirements
for the Degree of

Master of Engineering

in

CAD/CAM & ROBOTICS ENGINEERING

by

Paras Khullar

(821181007)

Under the supervision of

Mr. Satish Kumar
Assistant Professor



MECHANICAL ENGINEERING DEPARTMENT
THAPAR UNIVERSITY, PATIALA

July, 2014


CERTIFICATE

I hereby declare that the thesis entitled, "**Evaluation of Erosion Wear of Turbine Materials in Hydropower Plants**" is an authentic record of my work carried out as requirements for the award of degree of **Master of Engineering in CAD/CAM & Robotics Engineering at Thapar University, Patiala** under the supervision **Mr. Satish Kumar**, Assistant Professor, Mechanical Engineering Department, Thapar University, Patiala during July, 2011 to July, 2014. The matter embodied in this report has not been submitted to any other university or institute for the award of any degree.


Date: 18/07/2014



Paras Khullar

It is certified that the above statement made by the student is correct to the best of my knowledge and belief.


Mr. Satish Kumar
Assistant Professor
Mechanical Engineering Department
Thapar University Patiala-147004

Counter signed by


Dr. Ajay Batish
Professor & Head
Mechanical Engineering Department
Thapar University, Patiala


Dr. S.K. Mohapatra
Dean of Academic Affairs
Thapar University, Patiala

*Dedicated to
my
Respected Parents*

Acknowledgements

It is very rightly said that the best way to make your dreams come true is to wake up. This is a dream comes true for me while presenting this thesis at this point of my career. But as is for any other work of research, it would have not been possible for me without the guidance, inspiration and helping hand of so many kind human beings.

First of all with immense gratitude I acknowledge the support and help of **Mr. Satish Kumar, Assistant Professor, Mechanical Engineering Department, Thapar University, Patiala** who guided me throughout my work. It is because of his guidance and blessings I have completed my work successfully. I am grateful to **Dr. Ajay Batish, Head, Mechanical Engineering Department** who allowed me to use the facilities available in the department.

Also I would like to thank my parents who supported me in my difficult times and it is because of their blessings that I have completed this work.

At last I would like to thank Almighty God for making me able to write this thesis report.


PARAS KHULLAR

Abstract

Slurry erosion in hydro power plant turbine steels has proved to be a great problem from a long time. It mainly occurs due to the suspended sand particles in water which flows through the turbines of the hydro power plants which erode material of the turbine. This problem mainly occur due to heavy rainfalls specifically in monsoons days when a lot of sand particles come along the water.

To reduce slurry erosion it is necessary that some protective measures must be taken. So the need of the day is to manufacture the turbines with steels which resist slurry erosion to a great extent. Stainless steels have served a good purpose in this field and proved to be one of the best materials in this case. Moreover coatings done on the stainless steels prove the most effective method in improving resistance to slurry erosion.

The main aim of this work was to study the wear behaviour of different stainless steels with and without coatings in a slurry erosive environment. For this purpose three grades of stainless steels 304, 316 and 420 were used as substrate materials. A slurry of water and sand was prepared for this test. These were tested on a slurry pot tester with parameters of concentration 30 % and 50 %, speeds 1000 rpm, 1150 rpm, 1300 rpm and 1450 rpm of the rotating spindle and time at 80, 130 and 180 minutes on coated and uncoated samples. To improve the performance of these steels further these were coated with WC-17Co and Cr₂O₃ by the thermal spraying method of HVOF. The XRD and SEM analysis was also carried out on the eroded and uneroded samples. After the tests it was concluded that the coated samples resisted erosion greater than the uncoated samples. Performance of WC-17Co coatings proved to be the best followed by Cr₂O₃ coated samples.

Contents

Topic	Page No.
List of figures	viii
List of tables	xi
Nomenclature	xii
CHAPTER 1	
INTRODUCTION	1
1.1 Wear	1
1.2 Types of wear	2
1.2.1 Abrasive wear	2
1.2.2 Adhesive wear	2
1.2.3 Erosive wear	3
1.2.4 Surface fatigue wear	3
1.2.5 Corrosive wear	4
1.3 Mechanisms of erosive wear	4
1.3.1 Cutting erosion	4
1.3.2 Ploughing erosion	4
1.3.3 Platelet mechanism	4
1.3.4 Subsurface deformation and cracking	5
1.4 Parameters affecting erosion wear	5
1.4.1 Impact angle	5
1.4.2 Velocity of solid particles	5
1.4.3 Particle size and shape	5
1.4.4 Solid concentration	5
1.4.5 Hardness	6

1.5	Problem of slurry erosion in hydropower plants	6
1.6	Coatings	6
1.6.1	Electroplating	7
1.6.2	Physical vapour deposition	7
1.6.3	Chemical vapour deposition	8
1.6.4	Thermal spray coatings	8
	CHAPTER 2	
	LITERATURE REVIEW	12
	CHAPTER 3	
	PROPERTIES OF MATERIALS	24
3.1	Study of properties of sand	24
3.2	Base materials	24
3.2.1	Stainless steel 304	25
3.2.2	Stainless steel 316	25
3.2.3	Stainless steel 420	25
3.3	Coatings done on the base materials	26
3.4	X-Ray Diffraction	27
3.5	SEM analysis of the samples before erosion	31
	CHAPTER 4	
	EXPERIMENTAL SETUP	35
4.1	Description of slurry pot tester	36
4.2	Working procedure of slurry type pot tester	37
4.3	Description of workpiece sample	37
4.4	Parameters used in the test	38
	CHAPTER 5	
	RESULTS AND DISCUSSIONS	40
5.1	Comparison of erosion wear	40

5.1.1	Effect of erosion wear on uncoated base materials	40
5.1.2	Effect of erosion wear on WC-17Co coated materials	42
5.1.3	Effect of erosion wear on Cr₂O₃ coated materials	44
5.1.4	Comparison of erosion wear of uncoated and WC-17Co coated specimens at 30 % concentration	45
5.1.5	Comparison of erosion wear of uncoated and Cr₂O₃ coated specimens at 30 % concentration	47
5.1.6	Comparison of erosion wear of uncoated and WC-17Co coated specimens at 50 % concentration	49
5.1.7	Comparison of erosion wear of uncoated and Cr₂O₃ coated specimens at 50% concentration	52
5.2	SEM analysis of eroded samples	53
	CHAPTER 6	
	CONCLUSIONS	61
6.1	Conclusions	61
6.2	Future scope	62
	REFERENCES	63

List of figures

Figure 3.1	Vicker's microhardness tester	26
Figure 3.2	XRD results for Cr₂O₃ coated SS-304	28
Figure 3.3	XRD results for WC-17Co coated SS-304	28
Figure 3.4	XRD results for Cr₂O₃ coated SS-316	29
Figure 3.5	XRD results for WC-Co coated SS-316	29
Figure 3.6	XRD results for Cr₂O₃ coated SS-420	30
Figure 3.7	XRD results for WC-Co coated SS-420	30
Figure 3.8	SEM analysis of Cr₂O₃ coated SS-304 from cross-section at X200	31
Figure 3.9	SEM analysis of WC-17Co coated SS-304 from cross-section at X200	32
Figure 3.10	SEM analysis of Cr₂O₃ coated SS-316 from cross-section at X200	32
Figure 3.11	SEM analysis of WC-17Co coated SS-316 from cross-section at X200	33
Figure 3.12	SEM analysis of Cr₂O₃ coated SS-420 from cross-section at X200	33
Figure 3.13	SEM analysis of WC-17Co coated SS-420 from cross-section at X200	34
Figure 4.1	DUCOM Slurry pot tester	35
Figure 4.2	Parts of the slurry pot tester	36
Figure 4.3	Workpiece used in slurry type pot tester	38
Figure 5.1	Variation of wear (in mg) of uncoated SS-304 at 30% and 50% concentrations	40
Figure 5.2	Variation of wear (in mg) of uncoated SS-316 at 30% and 50% concentrations	41
Figure 5.3	Variation of wear (in mg) of uncoated SS-420 at 30% and 50% concentrations	41

Figure 5.4	Variation of wear (in mg) of WC-Co coated SS-304 at 30% and 50% concentrations	42
Figure 5.5	Variation of wear (in mg) of WC-Co coated SS-316 at 30% and 50% concentrations	43
Figure 5.6	Variation of wear (in mg) of WC-Co coated SS-420 at 30% and 50% concentrations	43
Figure 5.7	Variation of wear (in mg) of Cr₂O₃ coated SS-304 at 30% and 50% concentrations	44
Figure 5.8	Variation of wear (in mg) of Cr₂O₃ coated SS-316 at 30% and 50% concentrations	44
Figure 5.9	Variation of wear (in mg) of Cr₂O₃ coated SS-420 at 30% and 50% concentrations	45
Figure 5.10	Variation of wear (in mg) of uncoated and WC-Co coated specimens at 80 minutes and 30% concentrations	46
Figure 5.11	Variation of wear (in mg) of uncoated and WC-Co coated specimens at 130 minutes and 30% concentration	46
Figure 5.12	Variation of wear (in mg) of uncoated and WC-Co coated specimens at 180 minutes and 30% concentration	47
Figure 5.13	Variation of wear (in mg) of uncoated and Cr₂O₃ coated specimens at 80 minutes and 30% concentration	48
Figure 5.14	Variation of wear (in mg) of uncoated and Cr₂O₃ coated specimens at 130 minutes and 30% concentration	48
Figure 5.15	Variation of wear (in mg) of uncoated and Cr₂O₃ coated specimens at 180 minutes and 30% concentration	49
Figure 5.16	Variation of wear (in mg) of uncoated and WC-Co coated specimens at 80 minutes and 50% concentration	50
Figure 5.17	Variation of wear (in mg) of uncoated and WC-Co coated specimens at 130 minutes and 50% concentration	50
Figure 5.18	Variation of wear (in mg) of uncoated and WC-Co coated specimens at 180 minutes and 50% concentration	51
Figure 5.19	Variation of wear (in mg) of uncoated and Cr₂O₃ coated specimens at 80 minutes and 50% concentration	52

Figure 5.20	Variation of wear (in mg) of uncoated and Cr₂O₃ coated specimens at 130 minutes and 50% concentration	52
Figure 5.21	Variation of wear (in mg) of uncoated and Cr₂O₃ coated specimens at 50% concentration and 180 minutes	53
Figure 5.22	SEM analysis of Cr₂O₃ coated SS-304 surface at X500 and X1000	54
Figure 5.23	SEM analysis of WC-17Co coated SS-304 surface at X500 and X1000	55
Figure 5.24	SEM analysis of Cr₂O₃ coated SS-316 surface at X500 and X1000	56
Figure 5.25	SEM analysis of WC-17Co coated SS-316 surface at X500 and X1000	57
Figure 5.26	SEM analysis of Cr₂O₃ coated SS-420 surface at X500 and X1000	58
Figure 5.27	SEM analysis of WC-17Co coated SS-420 surface at X500 and X1000	59

List of Tables

Table 3.1	Properties of sand	24
Table 3.2	Micro hardness of samples	27
Table 4.1	Parameters used in the test	38

Nomenclature

<i>Co</i>	Cobalt
<i>WC</i>	Tungsten Carbide
<i>Cr₂O₃</i>	Chromium Oxide
<i>mg</i>	milligrams
<i>μm</i>	micrometers

Abbreviations

<i>SS-304</i>	Stainless Steel 304
<i>SS-316</i>	Stainless Steel 316
<i>SS-420</i>	Stainless Steel 420
<i>PVD</i>	Physical Vapour Deposition
<i>SEM</i>	Scanning Electron Microscopy
<i>XRD</i>	X-Ray Diffraction
<i>HVOF</i>	High Velocity Oxy Fuel
<i>D-Gun</i>	Detonation Gun

Chapter 1

Introduction

Water energy has been the most widely used form of renewable energy for the production of electricity. With today's emphasis on environmental considerations and conservation of fossil fuels, other renewable resources are being used to employ the energy sources of the sun and the earth for electricity generation. These resources, especially solar power, wind power and hydro power, have the capability to produce sustainable energy indefinitely with no direct emission of pollutant and greenhouse gases.

Hydropower is considered to be a renewable energy source because it uses the continuous flow of water without using up the water resource. It is also non-polluting, since it does not rely on burning fossil fuels. Hydropower is currently the leading renewable energy source in the world. In 2009, it accounted for about 63 percent of all other renewable energy sources, such as wind, solar, and biomass.

These generate electricity by utilizing the kinetic energy and potential energy of water which run the electric generators. Water coming from high mountains possess potential energy. As it flows down the mountains the potential energy of the water gets converted into kinetic energy resulting in high speed of the water. After passing through the turbine, the water re-enters the river on the downstream side of the dam. This water in turn strikes the blades or impellers of the turbines which generate electric power. For this purpose water coming from natural lakes or rivers can be utilized. It can also be stored in the dams during rainfall. Hydro power is a renewable source of energy which does not cause pollution or any other harm to the environment.

1.1 Wear

Wear is defined as the process of loss of material due to relative motion between two surfaces in contact with each other. Erosion wear is generally caused due to interactions between surfaces and the removal and deformation of material on a surface as a result of mechanical action of the opposite surface. Corrosive wear is caused due to interaction between the surfaces

chemically resulting in chemical reaction between them and destruction of one surface. Some other kinds of wear are discussed below.

1.2 Types of wear

- Abrasive Wear
- Adhesive Wear
- Erosive Wear
- Surface fatigue wear
- Corrosive Wear

1.2.1 Abrasive wear

When material is removed from the surface of a soft material by a harder material, it is known as abrasive wear. It leaves behind the hard particles of debris after the wear occurs. The abrasives which are responsible for this kind of wear can be some hard particles like sand particles or can be done by the other harder surface. In other words the abrasive wear can be defined as a process in which asperities of the harder surface dig into the softer one and makes grooves in the latter. Abrasive wear may be reduced by the use of lubricants of suitable thickness to separate the two surfaces and to wash out the solid particles in contact with the surfaces.

1.2.2 Adhesive wear

Adhesive wear is caused due to sliding under pressure between the two asperities which lock each other due to bonding because of adhesive forces between them. This is also called galling or scuffing. Plastic deformation of the surface takes place due to this type of wear as the yield stress is exceeded. This type of wear takes place due to absence of lubricants, due to which the junctions form a bonding between each other. This also leads to the removal of the surface which in addition again becomes wear particle and destroys the surface. The problem of adhesive wear can be overcome by the use of a suitable lubricant.

1.2.3 Erosive wear

It is the process of removal of material from a surface due to impact of a particle in a fluid flowing over the surface at high velocity. This impact of the solid particle transfers kinetic energy to the surface. More the velocity of the particle, higher will be the erosion. This is the main problem in fields like hydropower plants in which the turbine blades are affected with erosion as the water carries sand particles with it during monsoons. Another example can be ash disposal systems in various industries and thermal power plants which erode pipes and pump materials. The erosive wear mainly depends upon parameters like, impact angle, velocity of solid particles, particle size and shape and solid concentration. Types of erosive wear are:

- **Cavitation erosion** occurs when a solid and a fluid are in relative motion, and results in the formation of bubbles as the fluid becomes unstable and implodes against the surface of the material. It mainly occurs in marine applications such as propellers, turbines, etc.
- **Liquid impingement erosion** is caused due to repeated impacts between the surface and small liquid bodies distinct in nature which generate impulsive contact pressures on the former. As a result yield strength and endurance limit of the material is exceeded which destroys the material.
- **Solid particle erosion** occurs in a fluidic medium containing solid particles. It takes place when hard particles suspended in a fluid strike on the solid surface at high velocity and erodes the surface.
- **Slurry erosion** occurs when a slurry of some liquid and solid particles flows over the surface of a material at high speed. The solid particles suspended in the slurry strike over the surface at high velocity and as a result removes the material on the surface.

1.2.4 Surface fatigue wear

Stresses caused by periodic motion of mechanical machinery which leads to fatigue. The stresses in rolling and sliding contact fails the material due to fatigue. This occurs because of stresses below the surface. It causes micro-cracks leading to breaking of the surface. It starts below the surface where shear stress is maximum and reaches the surface gradually. Fatigue wear basically depends upon how many times the surface gets loaded and for how long it has been subjected to the same.

1.2.5 Corrosive wear

It is basically caused due to the chemical reaction of the surface of the material with the working environment of the erosion. The surface of the material reacts with the fluid and causes the weakening of the surface. When the surface is then subjected to cyclic loading, the surface acquires many cracks due to this weakening. Gradually with application of loads it starts breaking and erosion starts taking place. It is to be noted that erosion and corrosion are separate processes but they almost occur together in all the slurry erosive environments.

1.3 Mechanisms of erosive wear

Various mechanisms of erosive wear are:

- Cutting erosion
- Ploughing erosion
- Platelet mechanism
- Subsurface deformation and cracking

1.3.1 Cutting erosion

It takes place when the particles impacting are very sharp. When particles impact on the surface micromachining action takes place on the material and the material is removed. This mechanism is seen in almost all the erosion wears cases.

1.3.2 Ploughing erosion

This process is a two stage process in which plastic deformation of the surface takes place by particle impacts. First of all due to particle impact on the surface, it deforms plastically and a shear lip is formed. In the second stage due to repeated particle impacts this shear lip fails and breaks down due to fatigue.

1.3.3 Platelet mechanism

In this process when solid particle impacts on the target material, it spreads the target material in the direction of impact. This target material further flattens and extends to form a platelet. This mechanism is also known as extrusion.

1.3.4 Subsurface deformation and cracking

When a blunt particle strikes the target surface leading to its localized plastic deformation, which develops cracks on the surface which leads to brittle fracture of the material. This type of wear mechanism is known as subsurface deformation or cracking.

1.4 Parameters affecting erosion wear

These are the parameters on which erosion wear depend. These play an important role in the erosion wear of a material. These are defined as follows:

1.4.1 Impact angle

It is the angle between the direction of solid particle impinging on the surface and the plane of the surface. It is a major factor which affects the rate of erosion wear. But it highly depends upon the nature of surface on which the particle is striking.

1.4.2 Velocity of solid particles

It is the velocity of solid particles striking the target surface. The erosion rate is directly proportional to the velocity of solid particles. As the velocity of solid particles increase, their kinetic energy increases and hence they strike with more force on the material and cause erosion.

1.4.3 Particle size and shape

Particle size and shape is also a major factor in determining the erosion rate. The particles in the slurry can be of any type depending upon the nature of the latter. But it is seen that particles with sharp edges erode the material more readily.

1.4.4 Solid concentration

It is the amount of solid particles by weight or by volume present in the fluid. As the solid concentration increases the wear rate also increases as more solid particle come in contact with the surface. The concentrations can vary from 2% to 50% depending upon the nature of the slurry. At very high concentrations the velocity of particles striking the surface decreases as a result of increased particle interaction.

1.4.5 Hardness

The erosion wear highly depends upon the hardness of the target surface and the solid particles impinging on it. Hardness of the target surface can be defined as how readily it can resist permanent deformation with the impingement of solid particles on it. Hardness factor, which is the ratio of hardness of the target material to the hardness of the solid particles, determines the rate of erosion wear.

1.5 Problem of slurry erosion in hydropower plants

The hydro power plants suffer from a very big problem of slurry erosion as the sand particle flow along the water. The sand particles not only reduce the efficiency of the turbines but also destroy the turbine components. This problem mainly occurs due to heavy rains in the monsoons. The sediments formed by fragmentation of rocks and landslides also cause this problem. The material of the guide vanes is lost and erosion takes place. Also the problem is not only the erosion, but many other kinds of factors which harm the material in one way or the other. The material gets corroded very readily which weakens it and with successive flow of slurry it erodes the material. So the need of the day is to look after this serious problem and take necessary protective measures against the same. The material used should have proper strength and should not erode readily. Some features that the material should possess are high tensile strength, high hardness, resistance to corrosion, etc. If the material alone is not enough, a coating of suitable material should be applied on the substrate material to avoid erosion. Coating is a common measure taken into consideration for manufacturing of any part of even a simplest machine. Before coating a material it should be taken into consideration, for what purpose the coated material is to be used. If it has to be subjected to some solid particle erosion it should have high strength and if it has to be subjected to some corrosive environment the coating done must be of corrosion resisting features. Various types of coatings used these days are discussed below.

1.6 Coatings

There are many methods used for increasing the performance of the turbine materials. Coating is one of them. It is a process of spreading a layer of material over a base material to protect it

from damage like erosion, corrosion, etc. The base material over which the layer is spread is known as substrate. There are a number of techniques used for coating which are discussed as follows:

- Electroplating
- Physical vapour deposition
- Chemical vapour deposition
- Thermal spray

1.6.1 Electroplating

It is the process of changing surface properties of a material by deposition of a layer of some other material with the help of electric current. There are two materials dip into a solution known as electrolyte which carries metal salts. One of the material carries negative charge acting as a cathode and is the object over which coating is to be done. The other object carrying positive charge made up of material to be coated on the cathode acts as anode. When direct current is supplied to anode the metal ions are dissolved in the electrolyte and get deposited on the cathode. In this way the positively charged ions are reduced into metallic form.

1.6.2 Physical vapour deposition

It is the process of depositing thin films of metal in the vapour form on a substrate by its condensation. Very fine coatings of the order of 10 μm can be obtained by this process. The metal to be deposited is initially converted into vapour phase. Thereafter those vapours are allowed to be transferred on the substrate which then react with the latter to form a thin film of the coating.

Advantages

- It has excellent coating adhesion
- These coatings are more environment friendly

Disadvantages

- It is a technologically complex process
- Relatively very low thickness of the coatings are produced

1.6.3 Chemical vapour deposition

It is a process of depositing material from a gaseous phase by reaction on the heated substrate. Precursor gases are delivered into the reaction chamber at approximately ambient temperatures. As they come into contact with a heated substrate, they decompose forming a solid phase which and are deposited onto the substrate.

1.6.4 Thermal spray coatings

Thermal spraying is a process in which molten metal is deposited on a substrate by spraying. The coating particles are fed in powder or wire form, heated to molten state and sprayed on the substrate at high velocity in micrometer sized particles. Electrical arc discharge or combustion serve as the source of energy from thermal spraying. The sprayed particles are accumulated on to the surface of the substrate forming a layer of coating of the material. The quality of coating is measured in terms of its porosity, oxide content, macro hardness, surface roughness, etc. These are the coatings that are mostly used these days.

There are a number of thermal spray coatings

- Plasma spraying
- Detonation spraying
- Wire arc spraying
- Flame spraying
- High velocity oxy-fuel coating spraying (HVOF)

Plasma spraying process

It is process of depositing the material in powder or wire form by spraying it on the surface of the substrate with the help of a plasma torch at high temperature. High temperature of the material is achieved by exposing it to plasma flame which melts the material. This molten material is then accelerated towards the substrate. As the material comes in contact with the substrate, it cools down rapidly forming an adherent layer on it. The setup consists of spray gun which has an anode of nozzle shape made of copper and cathode made of tungsten material which are water cooled. Plasma gases such as argon, nitrogen, hydrogen, etc. flow through the

anodic nozzle around the cathode. A high voltage discharge initializes plasma causing localised ionisation and a conductive path for a DC arc between cathode and anode. The plasma initially is a neutral flame i.e. it does not carry charge. When the plasma is ready for spraying the electric arc extends down the nozzle. The cold gas around the anode nozzle narrows the plasma arc as it is electrically non-conducting which raises its velocity. As the powder is fed into the plasma flame, it is heated rapidly and accelerated towards the substrate resulting in very hard and strong coating.

Advantages

- These produce very dense and stronger coatings than other thermal spray processes
- It can work over very high temperatures and can be used to coat materials such as tungsten, ceramics, etc.

Disadvantages

- It is a complex process
- It is an expensive process

Detonation spraying thermal spray coatings

This set up consists of a gun known as Detonation Gun also known as D-gun. D-gun consists of a long water-cooled barrel which is closed at one end and open at the other. Oxygen and fuel gas is fed into the barrel together with coating material, which is in powder form and a spark is used to ignite the gas mixture. The resulting detonation heats and accelerates the powder to supersonic velocity through the barrel. A pulse of nitrogen is also used to purge the barrel after each detonation. This process is repeated many times in a second. The hot powder particles travel at a very high velocity of about 600 m/s towards the surface of the substrate. Due to high speed these particles possess very high kinetic energy which on impact produce very dense and strong coating on the substrate.

Advantages

- It is an economical process as compared to HVOF coating process.
- Coating material can be deposited at different rates varying from 50-110 grams/min

Wire arc spraying

It is a thermal spraying process in which where two consumable metal wires are fed independently into the spray gun. These wires are then charged and an arc is generated between them which melts the incoming wire. Then it is entrained in an air jet coming from the gun.

This molten material is deposited on the substrate and this process is known as Wire arc spraying. This process of coating is commonly used for heavy coatings.

Advantages

- Electric arc spray coatings are denser and stronger than other combustion spray coatings.
- It has high spray rates and high efficiency

Disadvantages

- The wires which are electrically non-conducting cannot be sprayed by this process.

Flame spraying

It is a process in which heat from combustion of a fuel gas, usually acetylene or propane with oxygen, to melt the spray coating material over the substrate. The coating material used is usually in powder or wire form. It is heated and propelled on to the substrate to form a surface coating.

Advantages

- These are used where the working conditions require a manual thermal spray coating
- It is cost effective

Disadvantage

- The quality of the coating is very poor

High velocity oxy fuel process

This process of coating was developed during the 1980's. In this process a mixture of gaseous or liquid fuel and oxygen is fed into a combustion chamber. Both of these are ignited and combusted continuously. Then through a converging-diverging nozzle the resultant hot gas flow at a pressure of 1 MPa and travels through a straight section. The fuels used can be gases like hydrogen, methane, propane, acetylene or liquids like kerosene, etc. The velocity of the jet at the exit of barrel is greater than the speed of the sound. A powder feed stock is injected into the gas stream, which accelerates the powder up to 800 m/s. The stream of hot gas and powder is directed towards the surface to be coated. The powder partially melts in the stream, and deposits upon the substrate. The coating has low porosity and high bond strength than any other type of coatings.

HVOF coatings may be as thick as 12 mm and is used for coatings such as ceramic and layers of metals, typically used in processes to resist wear and corrosion. Common powders used in this type of coatings are WC-Co, chromium carbide, alumina, etc.

Advantages

- Higher density, better wear resistance, tougher coatings, improved corrosion protection, higher hardness
- Higher strength bond
- Thicker coating due to less residual stresses
- Smoother as-sprayed surface due to higher impact velocities and smaller powder sizes

Disadvantages

- HVOF spraying usually needs to be undertaken in a specialised thermal spray booth, with suitable sound attenuation and dust extraction facilities.
- HVOF equipment requires more investment than other thermal spraying processes, for example flame and arc spraying.

Chapter 2

Literature Review

Slurry erosion is a great problem in many fields like thermal power plant, hydropower plants, etc. Engineers have been working in this field from a long time and many remedies have been found to overcome this problem. Erosion wear depends upon a number of factors which if controlled can reduce great amount of wear in all the fields. Some of the work done by the engineers have been summarised in this chapter.

Tu et al. (1999) have studied slurry erosion of α -Ti and plasma-nitrided Ti. They carried the tests on a jet-in-slit rig. The parameter used was velocity of jet from 6.4 - 15.2 m/s. The α -Ti and plasma-nitrided Ti alloy substrates were coated by TiN coatings. Slurry taken was water and silica. They concluded that TiN coatings showed high erosion resistance than α -Ti substrate under the same test conditions. Also they found that perforation and fragmentation of TiN coatings occurred after which craters and flakes were formed at the centre and cutting and ploughing was found at outer regions of the scars.

Wheeler et al. (2005) have studied erosion wear on carbon steel. (AISI 1020). They carried out sand erosion tests on a slurry jet erosion tester. Three coatings in use for offshore gate valves, hard chromium, electroless nickel composite and two HVOF tungsten carbide coatings was applied on carbon steel (AISI 1020) substrates. The particle size of sand used was 135 and 235 μm and velocity of jet was 28 ms^{-1} . They compared the performance with a D-gun 86WC–10Co–4Cr coating that was currently used. They concluded that that the Diatec applied HVOF 86WC–10Co–4Cr coating was the more effective, representing an improvement in erosion resistance of more than 50% over the D-gun applied coating of identical nominal composition.

Dsouza et al. (2005) have studied the effect of corrosion and erosion-corrosion of austenitic (UNS S31603) and super duplex (UNS S32760) stainless steels. They prepared a slurry of 3.5% NaCl solution with silica sand concentrations of 200, 500 and 1000 mg/l. The other parameters that were taken are two temperatures (20 and 50 $^{\circ}\text{C}$) and impingement velocity kept was 17 m/s. They coated both the substrate materials with WC-Co-Cr by HVOF type of thermal spray

coating. This test was conducted on jet impingement tester and performance of coated and uncoated samples was compared. They analysed the results by electrochemical techniques and SEM. They concluded that material is degraded very fast due to corrosion and erosion corrosion both and these are very dominating factors.

Mann et al. (2006) have studied slurry erosion and corrosion behaviour of substrate materials X20Cr13, 17Cr–4Ni pH steel and Ti6Al4V. They carried out tests on jet impingement tester. The parameters kept for the test were angle of impingement kept was 60° with jet velocities from 15-20 m/s. The sand used was of –40 to +80 mesh. Coatings of WC10Co4Cr, Armcore ‘M’ Stellite 6 and 12 HVOF coatings, TiAlN PVD coatings with substrate materials X20Cr13, 17Cr–4Ni pH steel and Ti6Al4V titanium alloy along with conventional hard weld deposits of Stellite 6 and 21 were prepared. They carried out corrosion analysis as per ASTM B 117-73 for 100 h. They concluded that WC10Co4Cr HVOF along with TiAlN PVD coatings performed best in erosion testing followed by HVOF coating of Armcore ‘M’ material. For corrosion, Ti6Al4V, Stellite 6 and 21 hard weld deposits and 17Cr–4Ni pH steel performed the best.

Maiti et al. (2007) have studied the improvement of the hardness of WC based HVOF coatings due to addition of WC powder to commercially available WC powders. These were tested as per ASTM standards for dry sand abrasion and slurry erosion. They found that 20% addition of WC powder improved the hardness of HVOF coating from 1106 to 1395 Hv0.3 which was due to embedding of WC hard metal matrix. They analysed the results and found that the erosion resistance of the coatings decreased with the addition of WC. They carried out SEM studies which showed that the porosity of the HVOF coating was higher than the conventional HVOF coating. They concluded that with increase in WC content (30%), the porosity of the HVOF coating increased up to 10% and hence the performance of the coated samples was decreased.

Sidhu et al. (2007) have studied the solid particle erosion behaviour of boiler tube steels (GrA1). The study was conducted, using an air jet erosion test rig. The parameters kept for the test were velocity of 26 m/s and impingement angle of 30° and 90° at 250 °C. Coatings of HVOF deposited NiCr and Stellite-6, coatings on boiler tube steels. The coatings were harder as compared to substrate steel. They analysed the surface of the material by method of Scanning

electron microscopy (SEM). They concluded that Mass losses of the coatings were found marginally higher than the boiler tube steel.

Santa et al. (2007) have studied slurry erosion testing of AISI 304 steel and AISI 431 steel. The testing apparatus used was a modified centrifugal pump. Slurry used was of distilled water and quartz sand particles of diameter between 212 and 300 μm . Impact velocity of slurry was 5.5 m/s with solid contents of 10%. They used two coatings applied by oxy fuel powder (OFP) and wire arc spraying (WAS) processes onto sand-blasted AISI 304 steel and compared it with the results of AISI 431 and ASTM A743 grade CA6NM stainless steels. The coating adherence was studied according to ASTM C 633 standards. They studied the surface characteristics by SEM which showed intense plastic deformation in both coated and bare stainless steels, with little evidence of brittle fracture in the microstructure. They concluded that the coated samples showed less erosion than the uncoated samples.

Manisekaran et al. (2007) have studied the slurry erosion of hydro turbine steels, such as 13Cr-4Ni martensitic steels. Tester used was jet erosion tester. The parameters kept were angle of impingement and particle size. They modified 13Cr-4Ni steels with pulsed plasma nitriding and laser hardening. They showed that erosion wear with 150-300 μm size was twice compared to 150 μm size slurry particulates. Laser hardening showed better performance at all angles of impingement. Plastic deformation of the samples occurred mostly and caused material removal for laser hardened surfaces. Pulsed- plasma nitrided steels exhibited chip formation and micro-cutting.

Santa et.al (2009) have studied the cavitation erosion performance of martensitic stainless steel. The cavitation erosion resistance of the coatings was measured in a vibratory apparatus according to ASTM G32 standard. The tester used for slurry erosion tests a modified centrifugal pump as well as in a high velocity jet erosion testing machine. Nickel, chromium oxide and tungsten carbide coatings were applied by oxy fuel powder (OFP) process and chromium and tungsten carbide coatings were obtained by high velocity oxy fuel (HVOF) process. They analysed the microstructure of coatings by light optical microscopy (LOM) and scanning electron microscopy (SEM), as well as by X-ray diffraction (XRD). They found that slurry erosion resistance increased upto 16 times on thermal spray coatings. No effect on cavitation resistance was found on either of the samples. Microstructure revealed that material was removed by micro-cutting and microploughing as well as detachment of hard particles.

For cavitation studies, OFP coatings showed brittle fracture and microcracking, and in nickel-based coatings some ductile deformation was also observed. In HVOF coatings, detachment of small particles led to formation of pores in WC/Co coatings while in CrC coatings the main wear mechanism was brittle fracture of particles.

Girish R. Desale et al. (2009) have studied erosion wear of aluminium alloy (AA 6063). The tester used for this purpose was a slurry pot tester. They used eight different sized quartz particles. The size of the particles varied between 37.5 and 655 μm . The parameters used for the test were velocity of 3 m/s with orientation angle of 30° and 90° in a sand-water mixture of 20% concentration (by weight). They found that erosion wear increases with increase in mean particle size 200 μm and below this size for the range of parameters under this investigation. They concluded that there exists a threshold energy for the impacting particles. The threshold kinetic energy for different operating conditions were determined and its relation with the change in erosion mechanism was discussed.

Padhy et al. (2009) have studied erosion wear in turbine materials. The parameters used in this test were size, hardness and concentration of silt particles and velocity of flow. Properties of the base material of the turbine components and operating hours of the turbine on erosion in actual conditions were also taken as the other parameters. Effect of these parameters on erosion in actual conditions had been investigated experimentally. They carried out an extensive experimental study on a small scale Pelton turbine. Based on the experimental data collected for different parameters they developed correlations for wear rate of Pelton turbine buckets as a function of critical parameters, i.e., size and concentration of silt particles and jet velocity.

Guanghong et al. (2010) have studied the corrosion-erosion wear behaviors of austenitic stainless steels, 316L and 13Cr24Mn0.44N in water-sand slurry and saline-sand slurry, respectively. They measured corrosion-erosion wear mass-loss to evaluate the influence of medium and materials. They analysed the worn surface and corrosion-erosion wear mechanism by scanning electron microscopy and a non- contact optical profilometer. Results showed that the corrosion-erosion wear mass-loss of 13Cr24Mn0.44N is lower than that of 316L in both the slurries. The relative wear resistance increased with the increasing of the impingement velocity and arrives at maximum of 1.6. The wear mechanism of 13Cr24Mn0.44N is abrasive wear in the water-sand slurry and it shows abrasive and corrosive behaviour both in saline-sand slurry. As the impingement velocity was increased, all the synergism ratios exhibited a

tendency of increase, among which the synergism ratio of 13Cr24Mn0.44N is always lower than that of 316L at any given velocity. They concluded that 13Cr24Mn0.44N possessed a predominant anti-corrosion-erosion wear property

Lee et al. (2010) have studied the wear resistance of S45C steel. They mixed powders with various particle sizes and studied their effect on the fracture toughness and wear resistance of thermally sprayed WC–10Co–4Cr coating layers fabricated by the HVOF (High-Velocity Oxygen Fuel) process on a S45C steel substrate. In order to obtain a high fracture toughness and wear resistance, the powder size and powder mixing ratio were varied. The microstructure and chemical composition of the phases in the coatings were characterized by means of the SEM and XRD techniques. Images were analysed for the evaluation of the porosity of the coatings. They also carried out hardness tests on the cross sections to evaluate the hardness and fracture toughness. The tester used for this purpose was a pin-on-disk wear tester at ambient temperature without lubrication. They concluded that mixing of a small amount of coarse powders with fine powders results in the highest fracture toughness and wear resistance, due to the formation of coating layers having the lowest porosity.

Liu et al. (2010) have studied wear and erosion behaviour of nano-WC–12Co powder addition in WC–10Co–4Cr AC-HVAF sprayed coatings on wear and erosion behaviour. In this work, nano-WC–12Co powder was added to the sub-micron WC–10Co–4Cr powder in order to improve the hardness of WC based AC-HVAF coatings. The result showed that 15% addition of nano-WC–12Co improved the hardness of AC-HVAF coating from 1677 to 1873 HV_{0.3} due to the embedding of nano-WC–12Co powder. They carried out sliding wear test and slurry erosion test were to evaluate the effect of adding nano-WC–12Co powder. They found that wear and erosion resistance of AC-HVAF coated samples go up with the addition of nano-WC–12Co powder, in addition, the coating hardness had also increased. They also carried out characterization tests of the coatings scanning electron microscopy (SEM), microhardness tester and X-ray diffractometer (XRD). Their results showed that the sample with 15% addition of nano-WC–12Co to WC–10Co–4Cr based AC-HVAF coating had the best wear and erosion resistance. They concluded that it is possible to fabricate the nanostructured WC–10Co–4Cr coating with low porosity and high hardness by AC-HVAF spray deposition with reasonable thermal spraying parameters.

Ramesh et.al (2011) have studied wear behaviour of mild steel. Mild steel was coated with thermally sprayed Inconel-718 coatings by APS process. Inconel-718 powder was thermal sprayed on mild steel substrate utilizing APS (air plasma spray) thermal spraying facility. Coatings of thickness 200 μm and 250 μm were produced by APS using powders of average particle size 50 μm . The developed coatings were slurry erosive wear in 3.5% NaCl media. They carried out microstructure studies and micro-hardness tests on the samples. Microstructural studies revealed uniformity of Inconel-718 coating with good bond and minimal porosities. SEM studies on the slurry eroded surfaces of both uncoated mild steel and Inconel-718 coating had been carried out. The surface hardness of developed coatings were higher than that of the substrate and increased with increase in coating thickness. They concluded that slurry erosive wear resistance of developed coatings were superior than that of uncoated mild steel substrate.

Jiang et al. (2011) have studied cavitation and jet impingement erosion on Inconel 600. The coating was deposited by cold spray method using pure Ni powder (60 wt.%) blended with α - Al_2O_3 (40 wt.%) as feedstock. Cavitation erosion (CE) experiments were carried out in the distilled water. Jet impingement erosion (JIE) experiments were performed in slurry containing 1 wt.% quartz particle. The parameters adopted were the flow velocity of 15 m/s at impingement angles of 30°, 60° and 90°, respectively. They observed the microstructure of the coating using optical microscope (OM) and scanning electron microscopy (SEM). Micro-hardness of the coating was determined by Vickers hardness tester. Cumulative mass loss vs. testing time was used to evaluate the erosion rate of the coating. The erosion mechanism was analyzed by OM, SEM, X-ray diffraction (XRD) and the micro-hardness measurement. Their results showed that the composite coating had compact microstructure and relatively high hardness. They concluded that the resistance to CE of the coating was not as good as that of Inconel 600 substrate due to the weak bonds of the Al_2O_3 particles. However, the results of the JIE test indicated that the slurry erosion resistance of the coating was better than that of Inconel 600 at the impact angles of 30° and 60°, but not at the normal impact angle.

Thakur et al. (2011) have studied slurry erosion behaviour of WC–CoCr cermet coatings deposited with two different WC grain sizes. Method of coating used was HVOF thermal spray. The tester used for this process was pot-type slurry erosion tester. They considered two parameters for testing erodent particle size and slurry concentration. They also studied surface morphology using SEM images and phase identification was done by XRD. They concluded

that WC–CoCr cermet coating deposited with fine grain WC exhibits higher slurry erosion resistance under all testing conditions as compared to conventional cermet coating.

Singh et al. (2011) have studied cavitation erosion hydraulic turbine components and suggested its mitigation by coatings. They gave an overview of the current state of understanding of cavitation erosion of materials used in hydro-turbines, coatings and coating methodologies for combating cavitation erosion, and methods to characterize cavitation erosion. They found that no single material property fully characterized the resistance to cavitation erosion but combination of ultimate resilience, hardness, and toughness rather may be useful to estimate the cavitation erosion resistance of material. They found that improved hydrodynamic design and appropriate surface engineering practices reduced damage due to cavitation erosion. The coatings suggested for combating the cavitation erosion encompassed carbides (WCCr₂C₃, Cr₃C₂, 20CrC-80WC), cermets of different compositions (e.g., 56W₂C/Ni/Cr, 41WC/Ni/Cr/Co), intermetallic composites, intermetallic matrix composites with TiC reinforcement, composite nitrides such as TiAlN and elastomers. A few of them had also been used commercially. Thermal spraying, arc plasma spraying, and high velocity oxy-fuel (HVOF) processes have been used commercially to apply the coatings. Boronizing, laser surface hardening and cladding, chemical vapor deposition, physical vapor deposition, and plasma nitriding have been tried for surface treatments at laboratory levels and have shown promise to be used on actual components.

Rajahram et al. (2011) have studied erosion-corrosion behaviour of UNS S31603. They studied the material response to incremental particle impact and evolution of surface and subsurface wear with time during erosion–corrosion. They performed multiple tests on a slurry pot erosion tester. The parameters used were time duration from 0.5 min to 2 h, 3.5% NaCl and 1 wt.% silica sand at a test velocity of 7 ms⁻¹. They also carried out SEM, FIB and TEM to investigate the mechanisms and microstructural changes that arise during this process. They found that between 0.5 min and 20 min of testing, when the particles are impacting the fresh uneroded surface, material removal occurs through the formation of prominent lips and deep craters. After a duration of 20 min, when the surface had been completely covered with a layer of lips and craters, a second layer started forming. Between 0.5 min and 20 min the depth of the nanocrystalline region formed subsurface increased with direct particle impact on the surface. They also found that nano and micro sized grains were formed as the top surface layer

became work hardened, load was transmitted by particle impact to the bulk grains. TEM investigation on the single particle impact crater revealed that deformed nanograins and twinning were formed immediately beneath the impact crater. TEM analysis of the specimen exposed to erosion–corrosion for 5 min also revealed the formation of deformed nanograins and twinning due to the high strain rates.

Singh et al. (2011) have studied the tribological behaviour of plasma sprayed conventional and nanostructured ceramic Cr_2O_3 –3% TiO_2 coatings. They used two testers pin on disc type dry sliding and pot type slurry erosion. Their experimental results indicated that there were two main wear mechanisms, plastic smearing and adhesive tearing, in the worn coatings under dry sliding. The concentrations of SiO_2 in water were selected to be 10, 20 and 30%. Particle size of SiO_2 particles was 75–106 μm . They found that the main damage in the coatings was due to formation and propagation of brittle cracks resulting in the detachment of coating surface material. They also carried out microstructural investigation to investigate the wear and erosion mechanism of the coatings using FE-SEM and EDS analysis. Also they studied properties like micro-hardness and porosity were also investigated for these coatings. They concluded that tribological performance of nanostructured coating was better as compared to plasma sprayed ceramic coating.

Yang et al. (2012) have studied the erosion-corrosion performance of X65 steel. The slurry used was oil sands slurry. Parameters used for the test were sand concentration, slurry flow velocity and impact angle. The tests were carried out on a jet impingement tester. Weight-loss test, polarization curve measurements and surface characterization were also carried out on the samples. They found that erosion components, including pure erosion and corrosion-enhanced erosion, were the dominant contributors to erosion-corrosion of the steel, while the contribution of corrosion components was slight. They concluded that with the increase of the sand concentration and slurry flow velocity, the erosion-corrosion rate of the steel increases however, an increasing impact angle decreases the erosion-corrosion rate of the steel in oil sands slurry.

Alegria et al. (2012) have studied the erosion–corrosion behaviour of SS-304. A multilayer CrN/Cr coating was produced by unbalanced magnetron (UBM) sputtering over AISI-304 stainless steel and its performance was compared with the performance of bare steel 304 using

the procedure indicated in ASTM G119-09. The results indicated that the total wear rate could be reduced by half with respect to bare stainless steel when this kind of coating is used. They found a strong reduction in the synergistic effect and pure corrosion effect for evaluated impact angles (30° and 90°) was similar. They concluded that the synergistic effect made the greatest contribution when bare steel was evaluated at 30°.

Goyal et al. (2012) have studied the slurry erosion behaviour of turbine steels. A high speed erosion test rig was used for slurry erosion tests and effect of three parameters namely average particle size, speed (rpm) and slurry concentration on slurry erosion of these materials was investigated. The CF8M turbine steel was coated with WC-10Co-4Cr and $\text{Al}_2\text{O}_3 + 13\text{TiO}_2$ coatings by the method of HVOF spraying and was subjected to slurry erosive environments. They found that the bare steel and $\text{Al}_2\text{O}_3 + 13\text{TiO}_2$ coating followed ductile and brittle mechanisms respectively under slurry erosion, whereas the WC-10Co-4Cr coating exhibited mixed behaviour (mainly ductile). They concluded that WC-10Co-4Cr coating was useful to increase the slurry erosion resistance of steel remarkably.

Amarendra et al. (2012) have studied the combined effect of slurry erosion and cavitation erosion under laboratory conditions. They analysed that material removal may occur by either of the modes or by their combined effect. They developed a simple method which combined both erosions as the damage is severe in this case. They used the setup of slurry pot tester and used triangular prismatic bluff bodies as cavitation inducers. They took brass test specimens and exposed them to water/slurry, with and without cavitation inducers. They concluded that there were significant variations in material loss confirming synergistic erosion damage.

Romo et al. (2012) have studied cavitation and slurry erosive performances of certain materials in laboratory. They compared the cavitation and slurry erosion resistances of Stellite 6 coatings and 13-4 stainless steel. The Cavitation Resistance (CR) was measured according to ASTM G32 standard and the Slurry Erosion Resistance (SER) was tested in a high-velocity erosion tester under several impact angles. Their tests showed that the coatings improved the CR 15 times when compared to bare stainless steel and SER of the coatings was also higher for all the impingement angles tested, the highest erosion rate was observed at 45°. They concluded that the main wear mechanisms were micro-cracking in cavitation tests, and micro-cutting and micro-ploughing in slurry erosion tests.

Rajkarnikar et al. (2013) have studied sediment erosion for hydraulic turbines. They developed a rotating disc apparatus for test of sediment-induced erosion in Francis runner blades. They considered the problem of sediment erosion caused in hydropower plants of Nepal. The hard abrasive material present in the river water of this region caused rapid erosion of turbine components and affected the performance of turbines, which in turn decreased the efficiency, reliability and operating life of such projects. Their study basically focussed at designing and developing of a laboratory test set up suitable for carrying out sediment erosion test in Francis runner blades. They developed a rotating disc apparatus which had been installed in Turbine Testing Laboratory, Kathmandu University, Nepal. In this laboratory Francis runner blades are used as test specimens. They concluded that the Francis turbines designed with traditional design methodology were highly prone to loss of material due to sediment erosion.

Arora et al. (2013) have evaluated the slurry erosion behaviour of a zirconium based bulk metallic glass, $Zr_{44}Ti_{11}Cu_{10}Ni_{10}Be_{25}$. They carried out slurry erosion tests using a non-circulating type test rig at impingement angles of 30° , 60° , and 90° . Commonly used hydro turbine steel was evaluated under the same test conditions. They found that at 30° impingement angle, the metallic glass demonstrated nearly 2.6 times higher erosion resistance compared to the steel. At normal impingement, the metallic glass was marginally better. At oblique impingement angles there were lower rates of erosion due to high hardness. For normal impingement, material was removed in the form of fragments from highly strained platelets due to limited plasticity of bulk metallic glasses. They concluded that hydro turbine steel showed ductile mode of erosion and metallic glass demonstrated a brittle mode of erosion with higher erosion rate at higher angle of impingement.

Grewal et al. (2013) have studied the erosion performance of turbine steels. They modified the surface of hydro turbine steel using friction stir processing. They improved bulk properties of light metals and their alloys by friction stir processing. They undertook commonly used turbine steel 13Cr4Ni for this process as turbine steels are susceptible to damage because of slurry and cavitation erosion. Microstructural characterization of the processed steel was conducted using optical microscopy (OM), scanning electron microscopy (SEM) equipped with energy dispersive spectroscopy (EDS), X-ray diffraction (XRD) and electron back scatter diffraction (EBSD) techniques. Mechanical characterization of the steel was undertaken in terms of micro hardness and resistance to cavitation erosion (CE). They refined the

microstructure with reduction in grain size by a factor of 10 by FSP. EBSD results confirmed the existence of submicron and ultrafine grained microstructure. After processing the microhardness of the steel increased by 2.6 times. The processed steel also showed 2.4 times higher resistance against cavitation erosion in comparison to unprocessed steel. They concluded that primary erosion mechanism for both the steels was identical in nature, with plastic deformation responsible for the loss of material.

Hong et al. (2013) have studied cavitation-silt erosion (CSE) behaviour of Cr_3C_2 -NiCr coating under different sediment concentration conditions. The coatings were done by high-velocity oxygen-fuel (HVOF) thermal spraying process. They found that Cr_3C_2 , Cr_7C_3 , Cr_2O_3 and (Cr, Ni) phases were obtained in the coating. The binder matrix contained amorphous phase and nanocrystalline grains. The crystallization temperature of the amorphous phase is about 559 °C. The coating exhibited low porosity and high microhardness. They observed that after eroding for 20 h, the CSE mass loss of the coating in $40 \text{ kg}\cdot\text{m}^{-3}$ was 1.15 and 1.23 times to that in $20 \text{ kg}\cdot\text{m}^{-3}$ and in $0 \text{ kg}\cdot\text{m}^{-3}$, respectively. Due to increase in interaction area of sand particles with specimen, the CSE rate was found to increase progressively as sediment concentration increases. They also observed signatures of lips, craters, microcutting, cracks and micropores on the eroded surface of the coating. They concluded that CSE mechanism for the coating is a composite ductile and brittle mode.

Ji et al. (2013) have studied the E-C behaviour of Zr55Cu30Ni10Al5 known as Bulk Metallic Glass (BMG). They carried out the tests on a slurry pot tester. Experimental results showed the volume loss rate of BMG increased with increase in the particle size, sand concentration or impact velocity. They also observed that the corrosion current density and the synergism rate increased with the increasing impact velocity. During E-C process, the surface microstructure transformed gradually from pure amorphous to composite mixture of crystalline and amorphous phases. They concluded that the E-C resistance of BMG is better than that of 304 stainless steel, but not as expected as its high hardness.

Cheng et al. (2014) have studied cavitation erosion on stainless steel and diamond like coating on it. They carried out all the tests on a rotating-disk test rig to explore the cavitation erosion resistance of the DLC coating. They examined mass losses, surface morphologies, chemical

compositions and the phase constituents of the specimens after cavitation tests are examined by using digital balance, scanning electron microscopy (SEM), energy dispersive spectroscopy (EDS) and X-ray diffraction (XRD), respectively. Their results indicated that the DLC-2 coatings elongated the incubation period of stainless steel, which lead to an excellent resistance to cavitation erosion as compared to the untreated stainless steel specimens. Plenty of scratches on stainless steel and damaged surfaces of stainless steel specimens were observed after 100 h duration of cavitation test. On the other hand only a few grooves and tiny pits are observed on the DLC-2 coatings. They concluded that decreasing micro defects and increasing adhesion reduced the delamination of DLC coating, and the erosion continued in the stainless steel substrate after DLC coating failure, and the eroded surface of the substrate was subjected to the combined action from cavitation erosion and slurry erosion.

Chapter 3

Properties of Materials

3.1 Study of properties of sand

Erosion of turbine blades is a big problem in hydro power plants all over the world. The main reason behind this problem is that during monsoons and heavy rains, a lot of sand come along with water flowing through the turbines and erode the blades of the turbine impellers. As the water sand slurry flows over the impellers it removes the material from it and leaves behind the surface redundant from the material. It also possess corrosive behaviour which corrodes the material making it weak which can be eroded with successive flow of slurry over it. Therefore it becomes necessary to study the properties of the sand so as to determine under what conditions it flows over the material. So the erodent material chosen was sand which was collected from Naptha Jhakri Dam. The 1500 MW hydro-electric power project is situated in Kinnaur district, Himachal Pradesh. Various properties of the sand were calculated as given below.

Table 3.1: Physical properties of sand, [Singh et al., 2011]

S.No	Name of the property	Value of the property
1	Specific Gravity	1.6
2	Particle Size	230 μ m
3	pH value of sand water slurry of 3% concentration	7.67
4	Static Settled Concentration	56.2% (initial concentration = 20% by weight)

3.2 Base materials

The selection of material used for the manufacture of turbines plays a very important role in their performance in different conditions. According to environment of hydro power plants the material of the turbine must possess the properties like high hardness, high tensile strength, high resistance to corrosion, etc. So stainless steels are considered to be suitable materials for

the use in manufacturing of turbines as they possess all the above mentioned properties. They also show resistance to solid particle erosion. Three grades of stainless steels were chosen properties of which are discussed below.

3.2.1 Stainless steel 304

SS-304 is a general purpose 18/8 stainless steel with good strength and excellent corrosion resistance. It is the most versatile and most widely used stainless steel, available in a wider range of products, forms and finishes than any other. It has excellent forming and welding characteristics. It has a balanced austenitic structure due to which it can be deep drawn without intermediate annealing. It is mostly used as turbine steels [Santa et al., 2007]. These are also used in industrial applications, architectural works, etc. It also possess excellent welding characteristics. It has a higher chromium and lower carbon content.

3.2.2 Stainless steel 316

SS-316 is an austenitic chromium-nickel stainless steel containing molybdenum. This increases corrosion resistance, improves pitting resistance from chloride ion solutions and increased strength at high temperatures. Its properties are similar to that of SS-304 except for its strength at elevated temperatures. It is a standard molybdenum grade steel which gives corrosion resistant properties than SS-304 and increases resistance to marine environments. It has excellent forming and welding characteristics. It has high creep strength at elevated temperatures and good heat resistance. It widely used in marine applications and as turbine steels [Goyal et al. 2012]. It can readily be formed into a variety of parts for applications in industrial, architectural fields.

3.2.3 Stainless steel 420

It is a martensitic stainless steel that provides corrosion resistance, increased strength and hardness. Grade 420 stainless steel is a high-carbon steel with a minimum chromium content of 12%. Like any other stainless steel, grade 420 can also be hardened through heat treatment. It is magnetic in both the annealed and hardened conditions. Maximum corrosion resistance is attained only in the fully hardened or fully hardened and stress relieved condition. This grade has the highest hardness among all the stainless steel grades with 12% chromium. It resists corrosion by the atmosphere, fresh water, mine water, steam, carbonic acid, crude oil, gasoline, perspiration, alcohol, ammonia, mercury, sterilizing solutions, soaps and other similar

corrosive media. Martensitic steels are used as turbine steels [Romo et al., 2012]. These steels are typically used in cutlery, surgical and dental instruments, scissors, etc.

3.3 Coatings done on the base materials

For the testing of erosion three materials SS-304, SS-316 and SS-420 were used on the tester. These materials as discussed above are very suitable materials for application in the blades of a turbine due to their high strength and corrosion resistance. But to increase their performance further two types of coatings were done on all the three materials. The coatings done were WC-17Co and Cr_2O_3 coatings. These coatings were done by the method of thermal spraying known as High Velocity Oxygen Fuel process as discussed earlier. Micro hardness of the samples with and without coating was checked on Vicker's Microhardness Tester in the Material Science laboratory at Thapar University, Patiala.



Figure 3.1: Vicker's Microhardness Tester

The values of hardness of the samples are as given in the below table.

Table 3.2: Micro hardness of the samples

S.No	Base Material	Coating	Hardness,Hv
1	SS-304	-	239
2	SS-316	-	256
3	SS-420	-	289
4	SS-304	Cr ₂ O ₃	551
5	SS-316	Cr ₂ O ₃	569
6	SS-420	Cr ₂ O ₃	613
7	SS-304	WC-17Co	839
8	SS-316	WC-17Co	915
9	SS-420	WC-17Co	1103

So as we can see from the above results micro hardness has varied from one material to the other. The micro-hardness of SS-420 coated with WC-17Co is found to be the highest among all the other materials. Hardness plays a very important role in the erosion wear of a material. Erosion resistance is directly proportional to hardness of the material.

3.4 X-Ray Diffraction

It is a tool which is used to identify the atomic and molecular structure of a crystal in which the crystalline atoms cause a beam of incident X-rays to diffract into many specific directions. A three-dimensional picture of density of electrons within the crystal can be produced by measuring their angles and their intensities. In this way mean positions of the atoms in the crystal, chemical bonding, disorder and various other informations can be determined. It is used in the characterization of the material by knowing its atomic structure. XRD of all the coated samples was carried out at the Sophisticated Analytical Instrumentation Laboratory, Thapar University Patiala. The results of the tests are as follows:

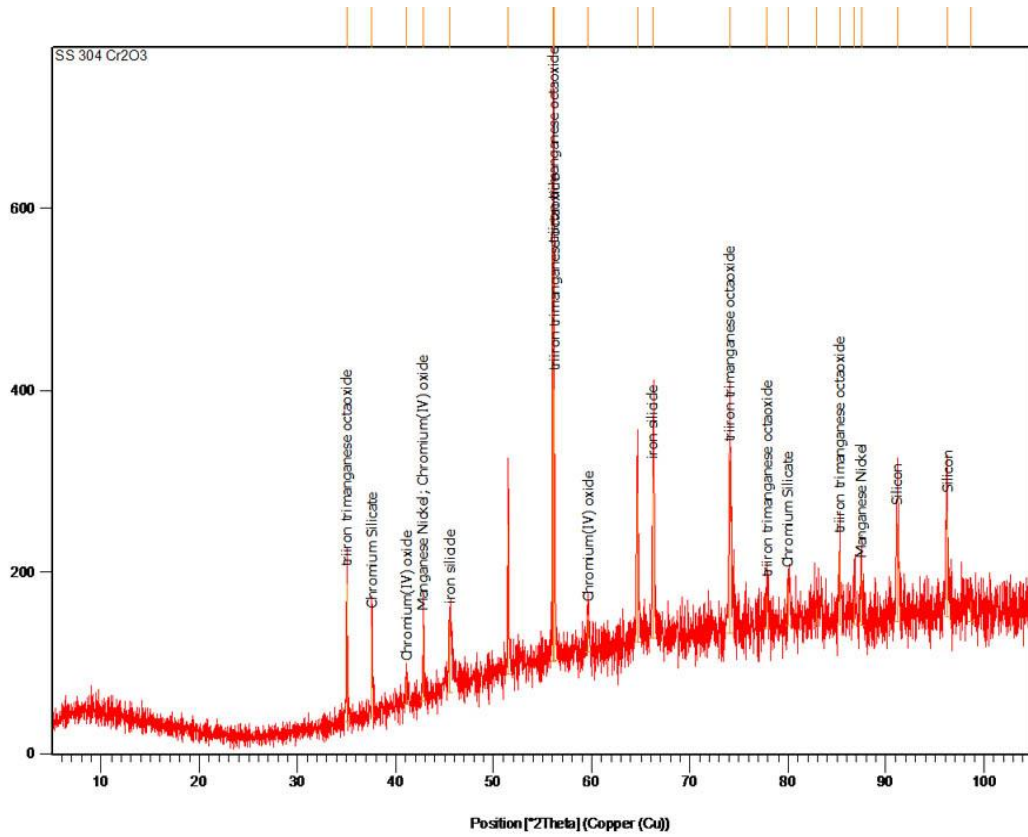


Figure 3.2: XRD results for Cr₂O₃ coated SS-304

The above figure shows the presence of chromium oxide in SS-304 material.

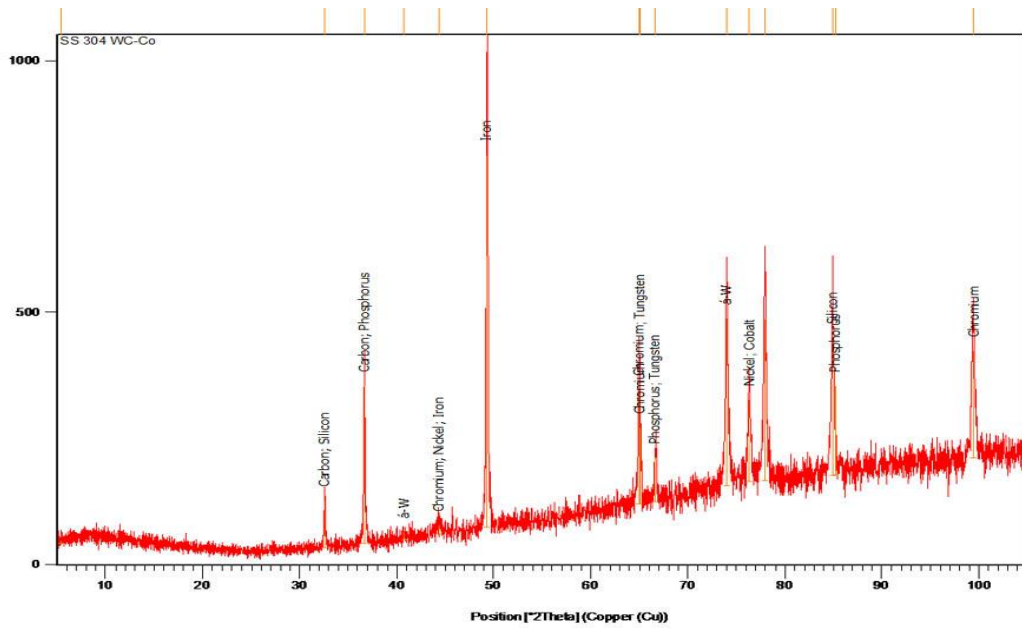


Figure 3.3: XRD results for WC-17Co coated SS-304

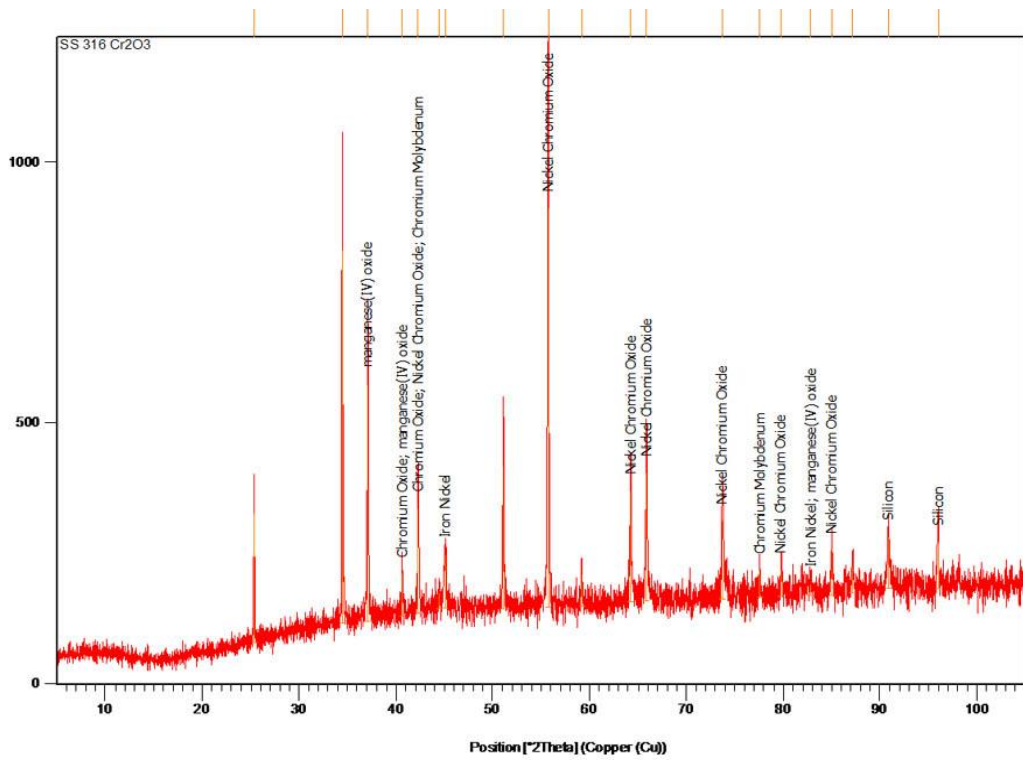


Figure 3.4: XRD results for Cr_2O_3 coated SS-316

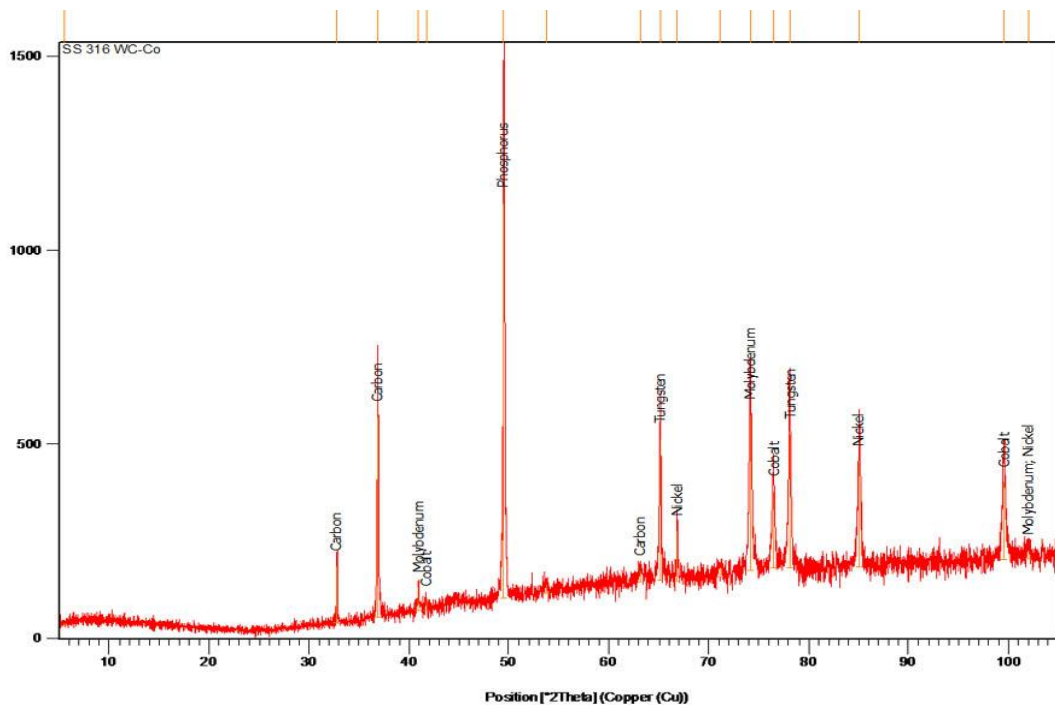


Figure 3.5: XRD results for WC-17Co coated SS-316

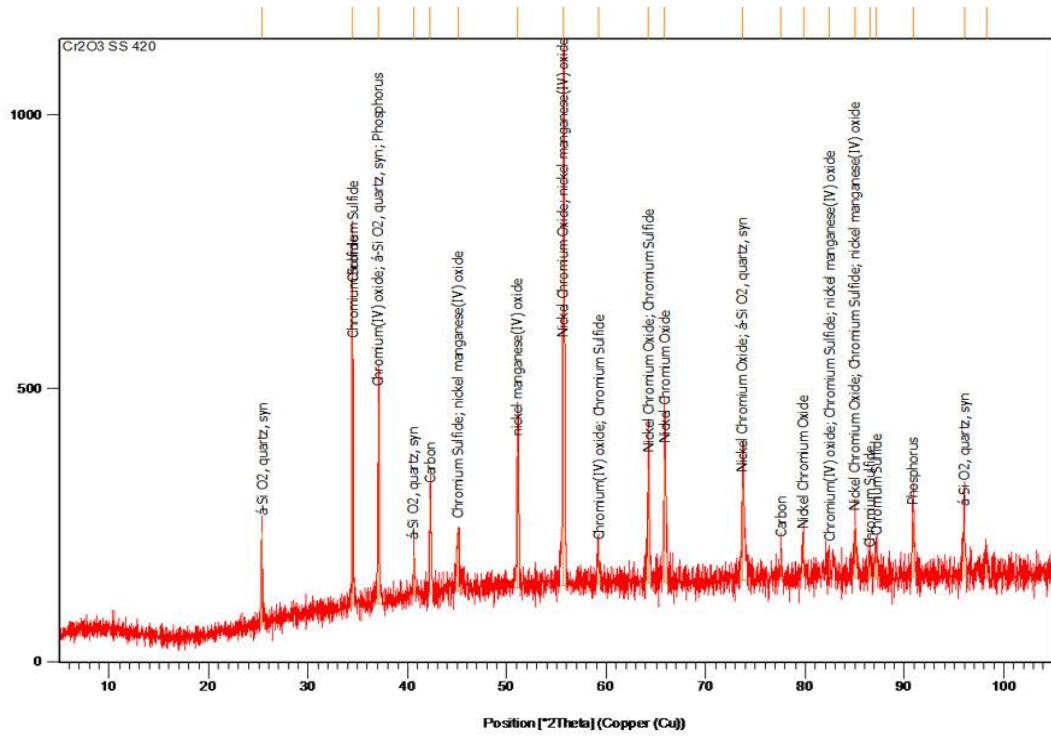


Figure 3.6: XRD results for Cr₂O₃ coated SS-420

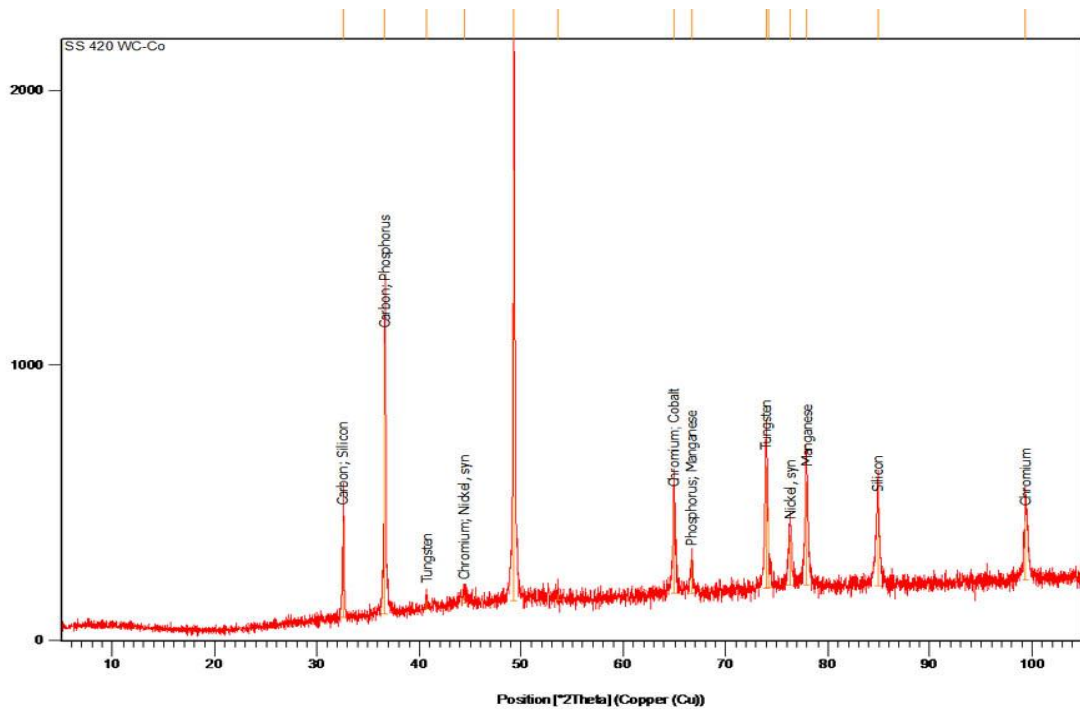


Figure 3.7: XRD results for WC-17Co coated SS-420

In figures 3.2, 3.4 and 3.6 clearly Cr_2O_3 can be seen in the peaks. The other materials present are that of the base metal. In figures 3.3, 3.5 and 3.7 WC-Co can be found in the samples which is responsible for the hardness of the sample.

3.5 SEM analysis of the coated samples before erosion

SEM is a microscopy that produces images of an object focussing a beam of electrons on it. It is because of the interaction of electrons with the atoms in the sample. It gives information regarding surface topography and composition of the sample. The SEM analysis was done at Sophisticated Analytical Instrumentation laboratory at Thapar University, Patiala. This test was done to see the bonding of coating with the substrate material.

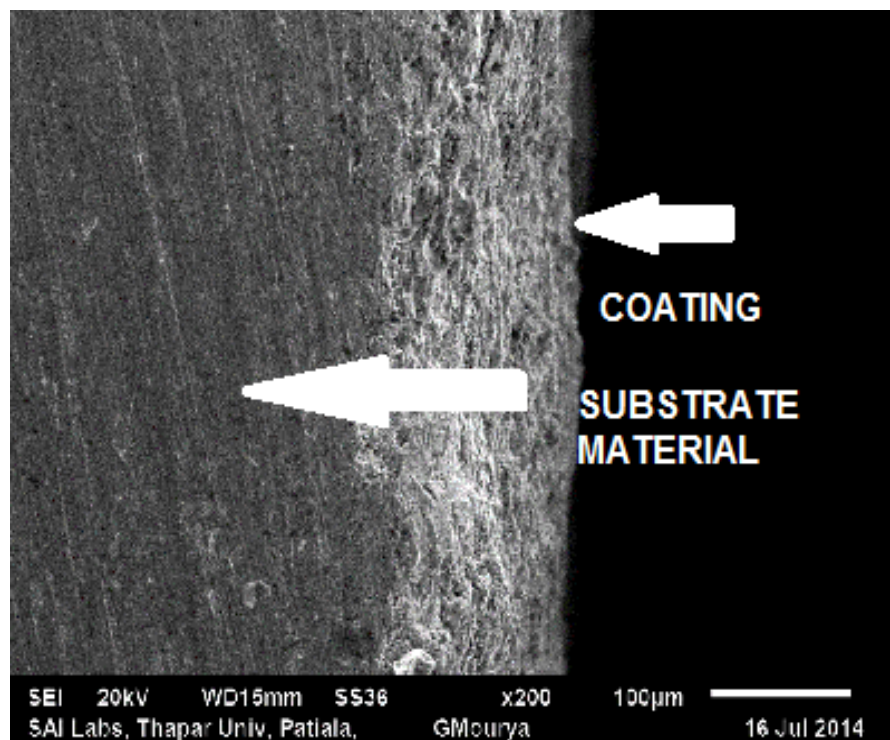


Figure 3.8: SEM analysis of Cr_2O_3 coated SS-304 from cross-section at X200

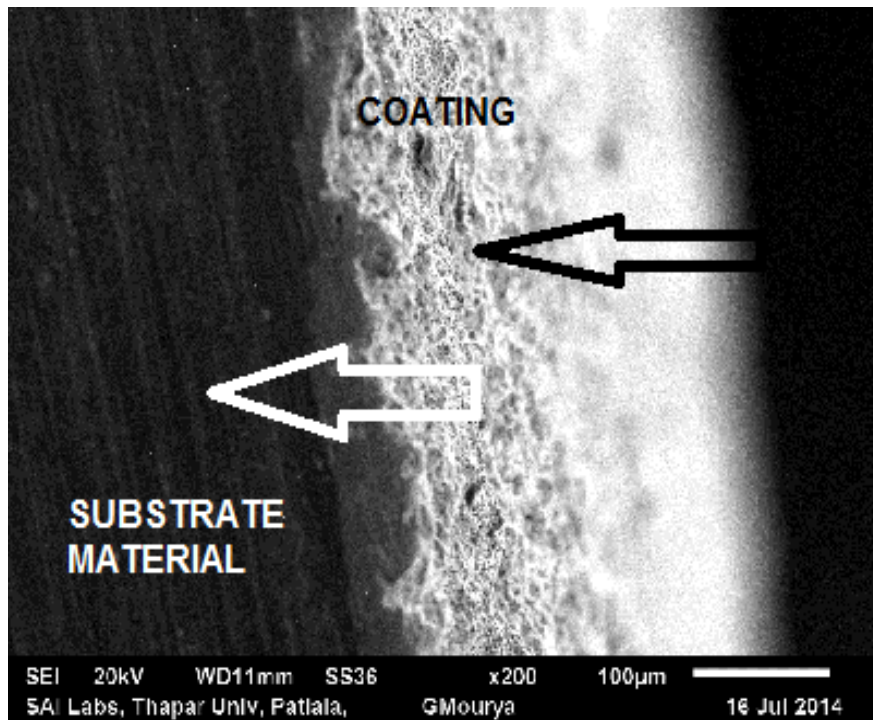


Figure 3.9: SEM analysis of WC-17Co coated SS-304 from cross-section at X200

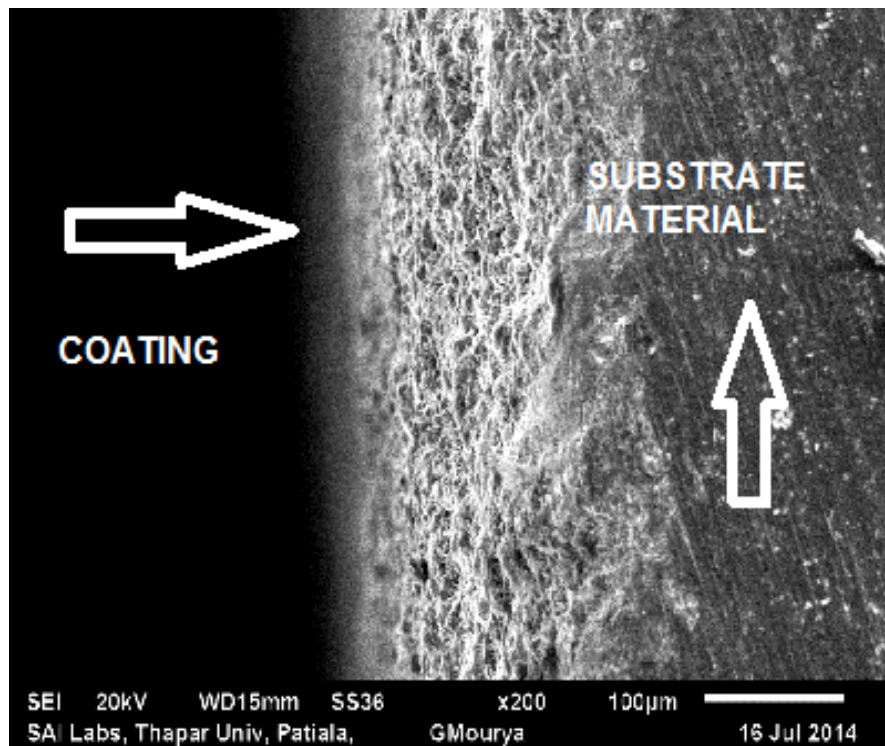


Figure 3.10: SEM analysis of Cr_2O_3 coated SS-316 from cross-section at X200

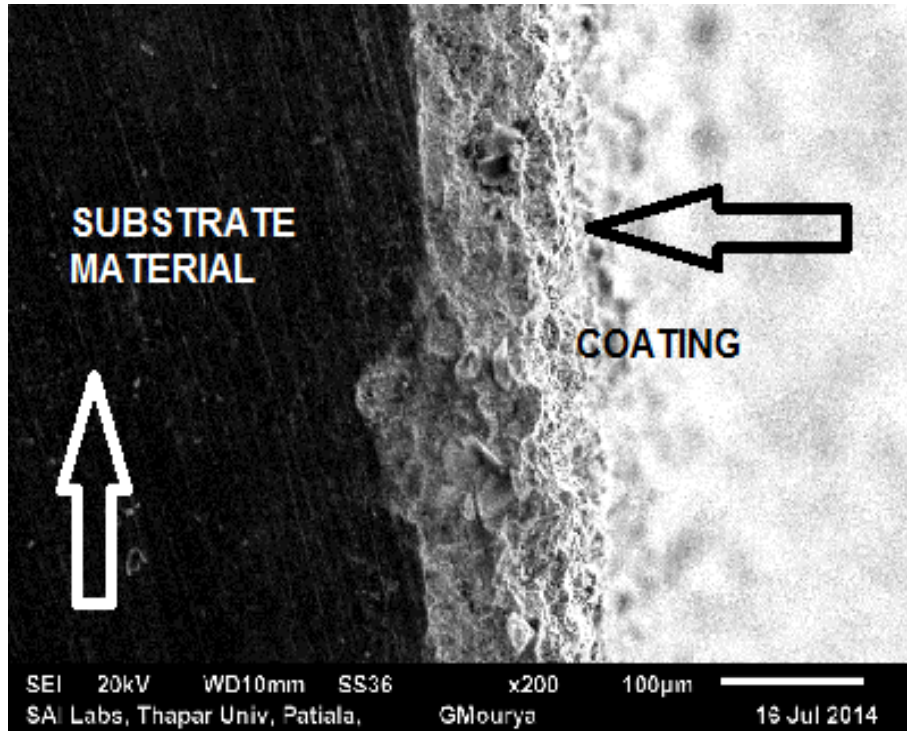


Figure 3.11: SEM analysis of WC-17Co coated SS-316 from cross-section at X200

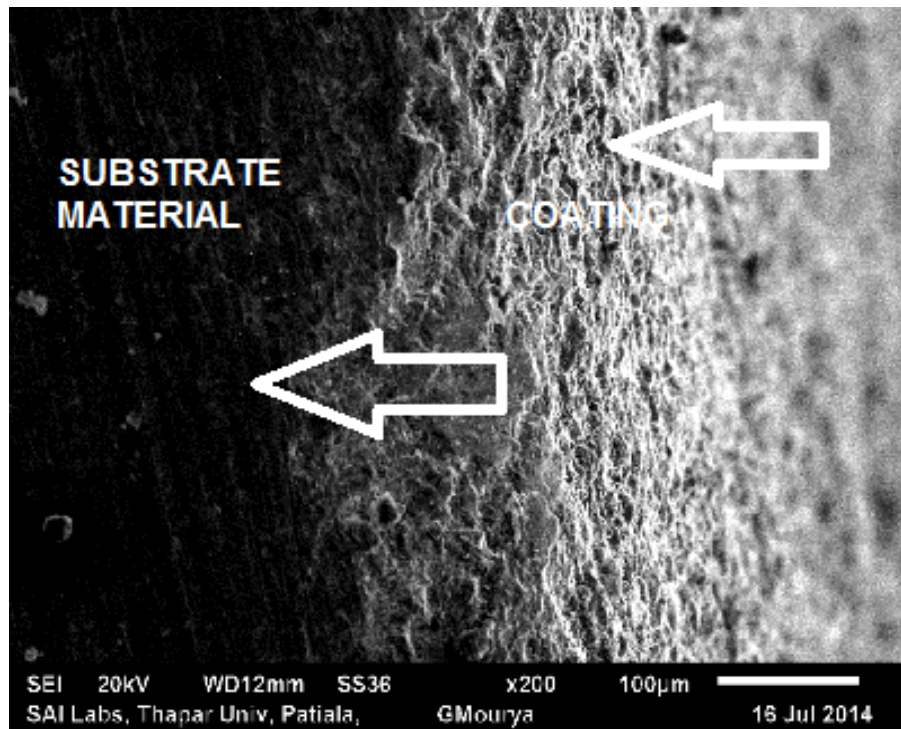


Figure 3.12: SEM analysis of Cr_2O_3 coated SS-420 from cross-section at X200

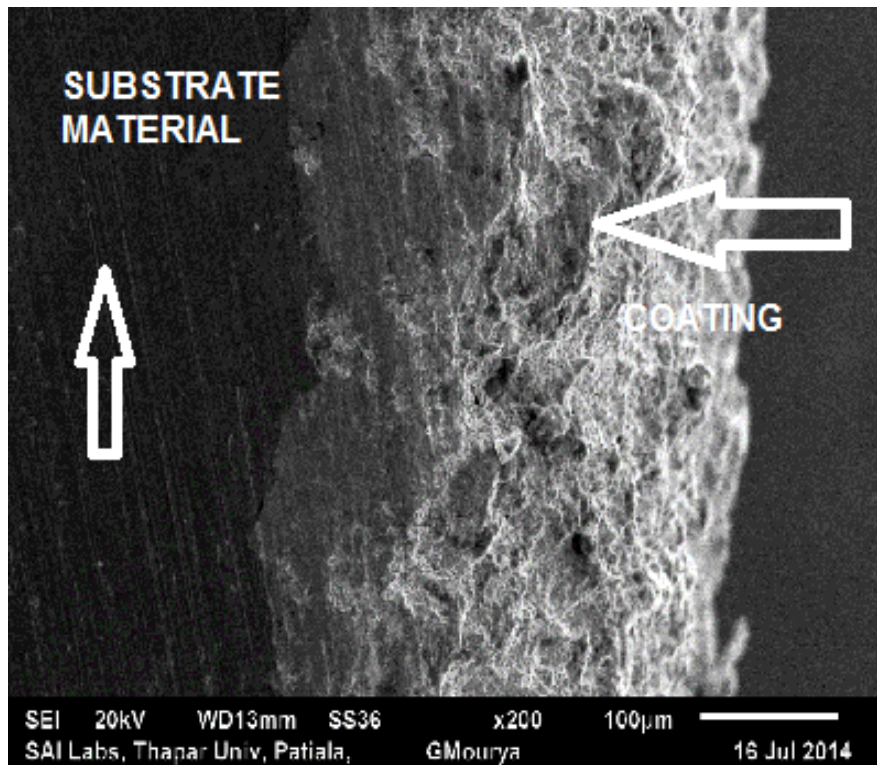


Figure 3.13: SEM analysis of WC-17Co coated SS-420 from cross-section at X200

All the above figures show strong bonding of the coating with the substrate material as we see it at X200 magnification.

Chapter 4

Experimental Setup

Slurry erosion is a serious problem as it limits the useful life of equipment and is therefore a critical parameter for design, selection and operation of the hydraulic transportation system. Engineering interest is to estimate the service life of equipment / components subjected to slurry erosion and to investigate the possibilities of enhancement of their life. A number of bench scale test rigs are available to evaluate the slurry erosion. Among the various selected test rigs, a Slurry Pot tester has been commonly used by several investigators. Other reasons for the selection of slurry pot type of test rig compared to others are:

- Different speeds of the specimen are possible.
- Time can be successfully set for a set of reading.
- Different concentrations of sand can be taken in the pot.



Figure 4.1: DUCOM Slurry pot tester

The Slurry Pot Tester is available at Thapar University, Patiala in the I.C. Engines lab.

4.1 Description of slurry pot tester



Figure 4.2: Parts of the slurry pot tester

The test rig consists of a Rotating Spindle, Cylindrical Pot, Propeller, Screw jack and Digital meter to set speed and time. The Rotating Spindle itself holds the work piece and propeller fixed to it. With the rotation of spindle the work piece and propeller also rotate with it. A propeller is fixed at the end of the spindle so that the sand particles do not settle down and may be suspended in the mixture throughout the working process. A slurry of sand and water with suitable ratio is prepared in the Cylindrical Pot. The pot is placed in the container/jacket so that the water may not spill out of the pot. The container is continuously supplied with cold water to cool the pot as with the operation the slurry becomes very hot. The Pot can be lifted up and

down with the help of a Screw Jack mounted at the bottom of the tester. During the operation the pot is at the top position and when the work piece is to be removed it has to be lowered with the help of screw jack. Two Digital Meters are available for setting up rotating speed of the spindle and the total number of revolutions per minute.

4.2 Working procedure for slurry pot tester

The working of a Slurry Pot Tester is based on the principle that as a slurry of some erodent material like sand flows over a piece of metal, it erodes its surface. This experiment follows the following steps:

1. Clean the pot and rinse it thoroughly with water so that any extra erodent material previously present in the pot may be removed.
2. Place the pot in the container on its seat.
3. Prepare a slurry of the erodent material and water mixed in some definite proportion.
4. Weigh down the specimen on a weighing machine of accuracy of 0.0001 g.
5. From the spindle remove the stirrer/propeller and fix the specimen along with the propeller at the bottom.
6. Lift the pot upwards with the help of the jack provided at the bottom.
7. Connect the inlet pipe of the container to a cold water supply and outlet to some drain. Start the supply of water.
8. Switch on the MCB.
9. Set the RPM by rotating the knob and enter the total number of revolutions for the specimen to rotate.
10. As we press on the start button the number of RPM's can be seen on the LED indicator.
11. After the completion of the revolutions the spindle stops rotating by itself.
12. Turn off the MCB and cut off the supply of cold water.
13. Lower down the pot and remove the specimen. Wash and clean it with water.
14. Measure the weight of the specimen on the same weighing machine.
15. Repeat the same from step 1. for another reading.

4.3 Description of the workpiece sample

Flat work pieces of all the 3 materials were made. The dimensions of the work piece are 25mm X 75mm X 5mm. It consists of a through hole at the centre to be held in the fixture. The

workpiece samples were prepared were prepared, grinded and finished properly. The hole was drilled in the samples.



Figure 4.3: Workpiece used in slurry type pot tester

4.4 Parameters used in the test

The 3 parameters used in the experiment are

1. Speed (in R.P.M)
2. Sand Percentage in water
3. Time

Table 4.1: Parameters used in the test

S.No.	Parameter	Variation
1	Sand Percentage in water	30%
		50%
2	Speed (in r.p.m.)	1000
		1150
		1300
		1450
3	Time (in minutes)	80
		130
		180

The above mentioned parameters are used to study the slurry erosion characteristics of SS-304, SS-316 and SS-420 samples. The samples coated were also subjected to same parameters and the erosion performance of coated and uncoated samples was studied and compared.

Chapter 5

Results and Discussions

The erosion tests were performed on slurry pot tester with different parameters of concentration, time and speed. The wear rate for all the parameters was calculated and compared by plotting graphs for all the parameters. The wear rate of the specimens with coating was also calculated. The results varied from one parameter to the other. All the results are discussed below in detail.

5.1 Comparison of erosion wear

Erosion wear of the samples is calculated on the basis of their mass loss in milligrams. All the uncoated and coated samples were weighed at weighing machine of 0.0001 accuracy. After calculating the wear of all the samples, they were plotted against the different speeds at which these were calculated. The results are as follows.

5.1.1 Effect of erosion wear on uncoated base materials

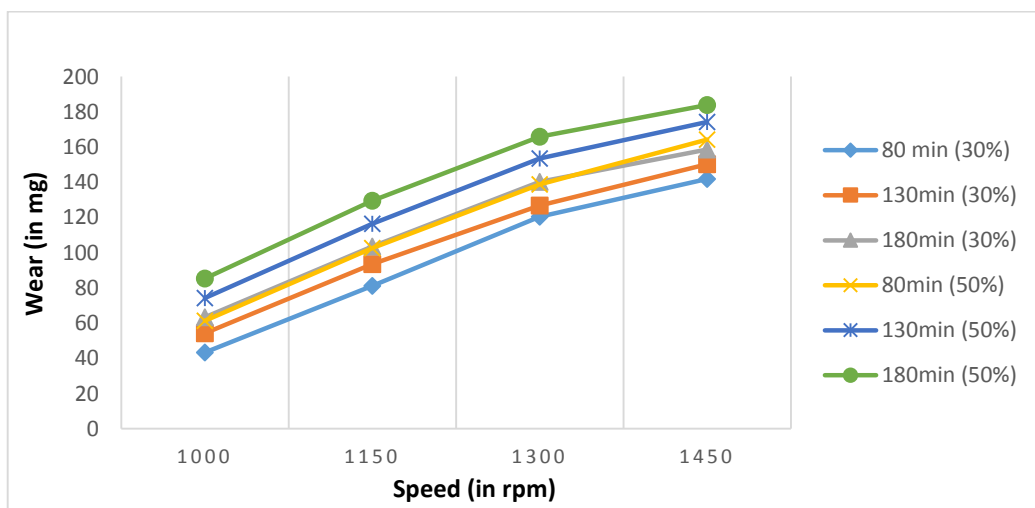


Figure 5.1: Variation of wear (in mg) of uncoated SS-304 at 30% and 50% concentrations

Figure 5.1 compares the wear taking place at two concentrations i.e. 30 % and 50 %. As we can see from the graph at same speeds the erosion wear increases with the concentration of the sand in water. Also it can be seen that the wear is directly proportional to speed. The trend of the graph shows that the wear of the material is minimum at lowest values of speed and concentrations i.e. 1000 rpm and 30 % respectively and on the other hand maximum at the highest values of speed and concentrations i.e. 1450 rpm and 50 % respectively. Wear increases gradually as the concentration and speed increases.

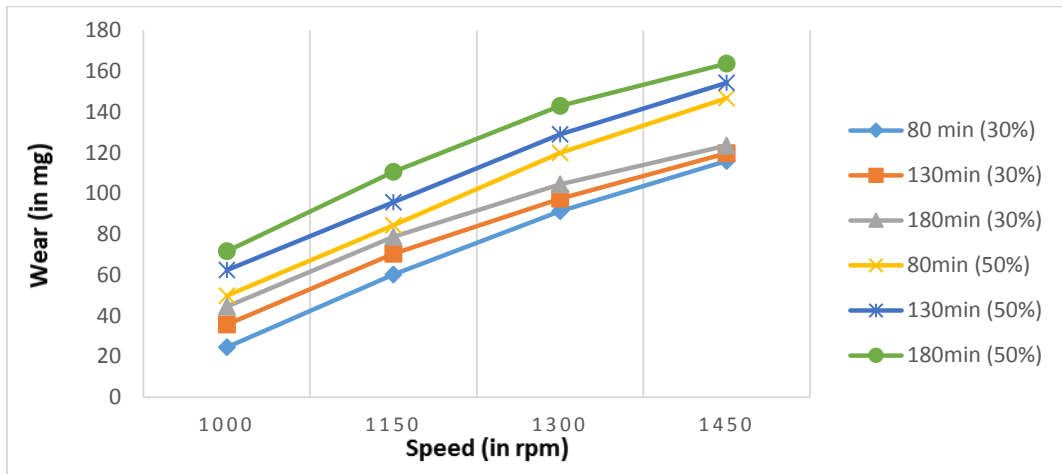


Figure 5.2: Variation of wear (in mg) of uncoated SS-316 at 30 % and 50 % concentrations

From figure 5.2 it is clear that erosion increases with concentration. However SS-316 showed less wear as compared to SS-304.

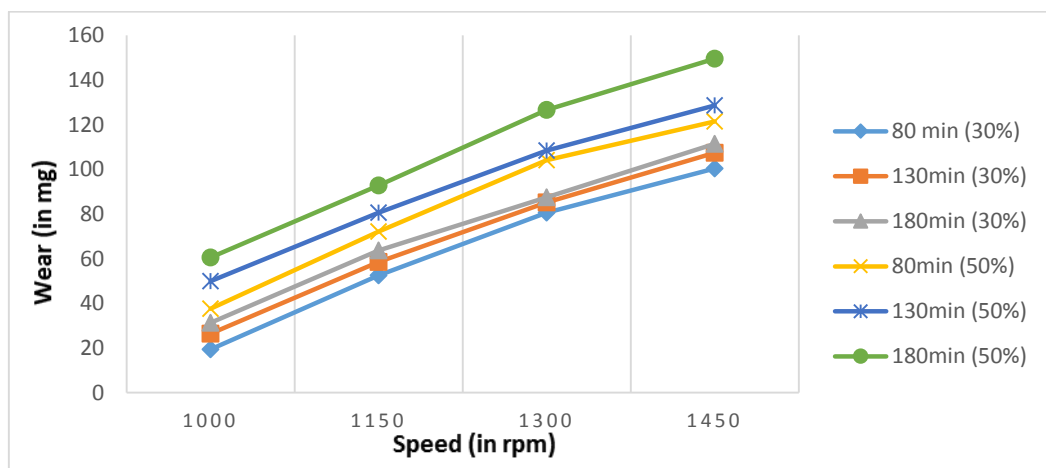


Figure 5.3: Variation of wear (in mg) of uncoated SS-420 at 30 % and 50 % concentrations

From the figures 5.1, 5.2 and 5.3 it can be seen that wear shows the decreasing variation (SS-420 < SS-316 < SS-420). It is because of wear resistant properties of the three materials. Although the trend of the graph is same in all the materials. Thus from the graphs it is clear that the wear increases with speed and concentration of sand. To increase the wear resistance further, coatings of suitable materials are needed to be done on the materials and again all the tests to be conducted at same parameters. It is shown in the below figures.

5.1.2 Effect of erosion wear on WC-17Co coated materials

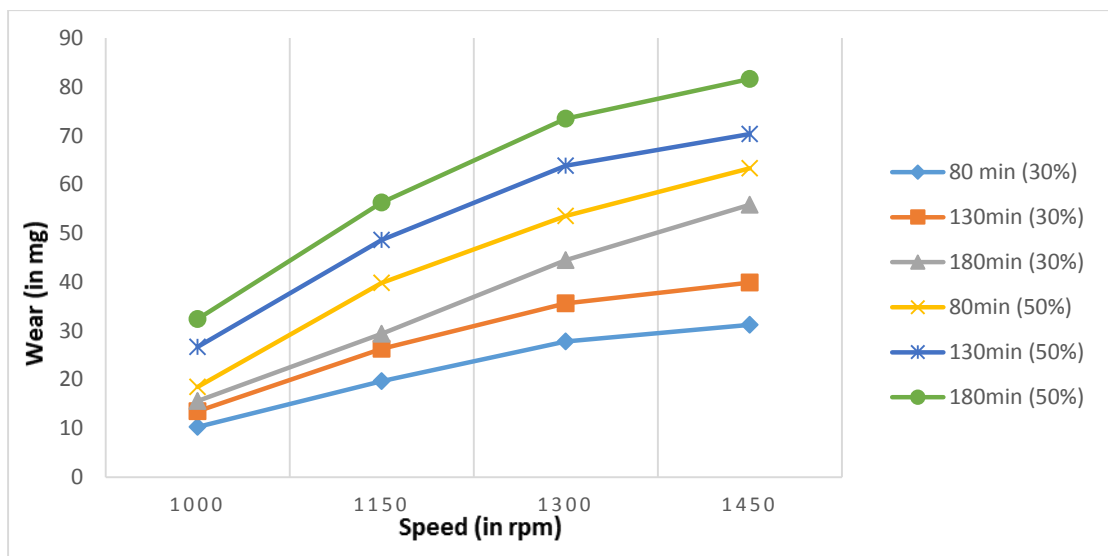


Figure 5.4: Variation of wear (in mg) of WC-17Co coated SS-304 at 30 % and 50 % concentrations

WC is a very hard element and possess excellent wear resistant properties as compared to any other available element. This is the most suitable material and is mostly used in hydro power plant turbines. As we compare figures 5.1 and 5.4 we can see a huge difference in the wear loss of the material. The same material under same parameters shows a considerable amount of decrease in the wear of the material after coating. Again the trend of increasing wear with increase in speed and concentration continues.

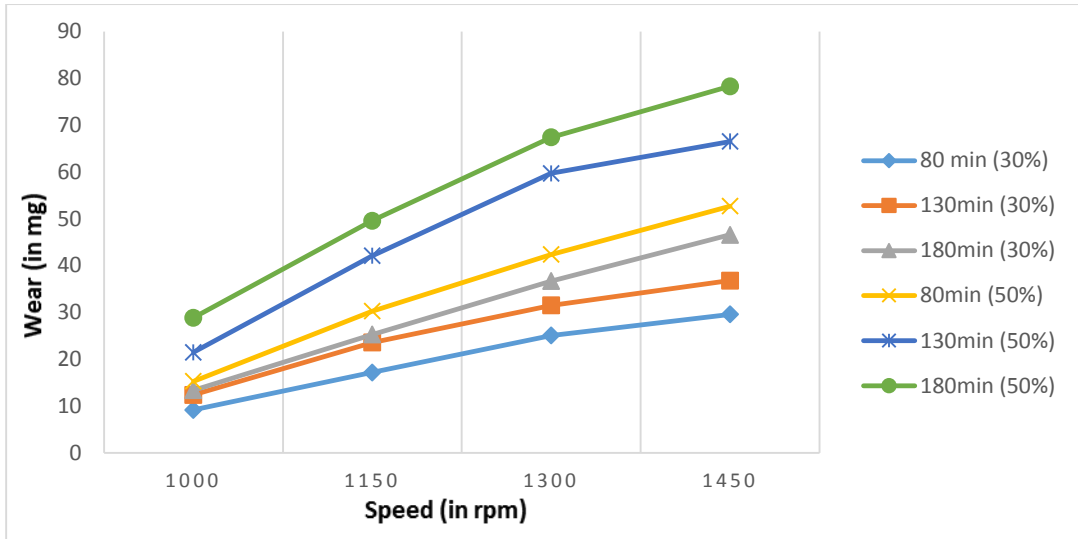


Figure 5.5: Variation of wear (in mg) of WC-17Co coated SS-316 at 30 % and 50 % concentrations

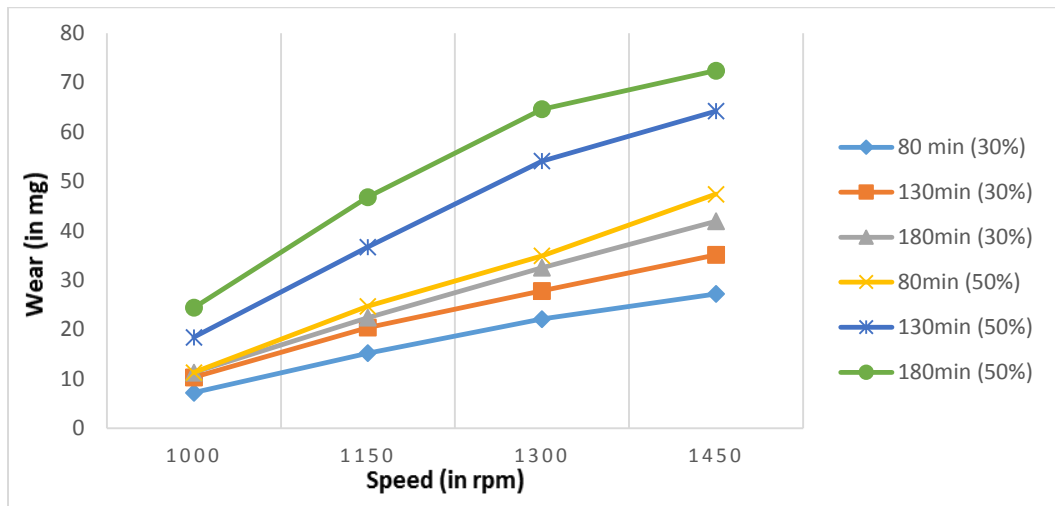


Figure 5.6: Variation of wear (in mg) of WC-17Co coated SS-420 at 30 % and 50 % concentrations

Comparing the figures 5.2, 5.3, 5.5 and 5.6 we can see the difference in wear loss with increasing hardness of the material. Thus WC-17Co coated SS-316 and SS-420 show a marginal resistance in wear loss of the material than uncoated samples but the trend remaining the same, more the concentration and speed, greater is the loss of material in wear however concentration being more dominant.

5.1.3 Effect of erosion wear on Cr₂O₃ coated materials

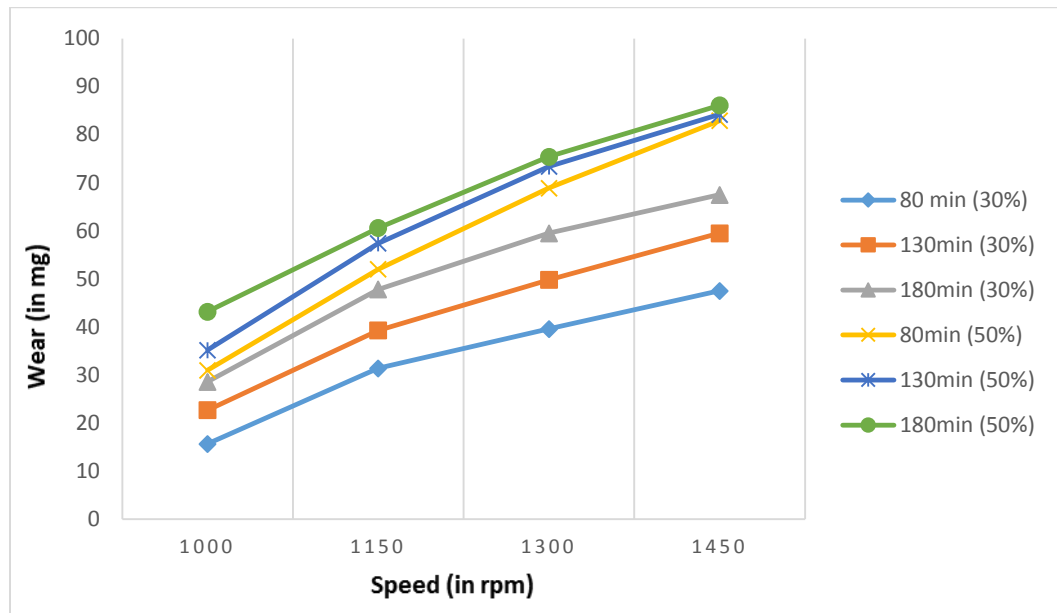


Figure 5.7: Variation of wear (in mg) of Cr₂O₃ coated SS-304 at 30 % and 50 % concentrations

The second coating material used was Cr₂O₃. It comes under the category of ceramic coatings. This coating also shows resistance to wear as compared to uncoated samples. It is clear from the figures 5.1 and 5.7 that coated specimen resisted wear loss more than the uncoated ones.

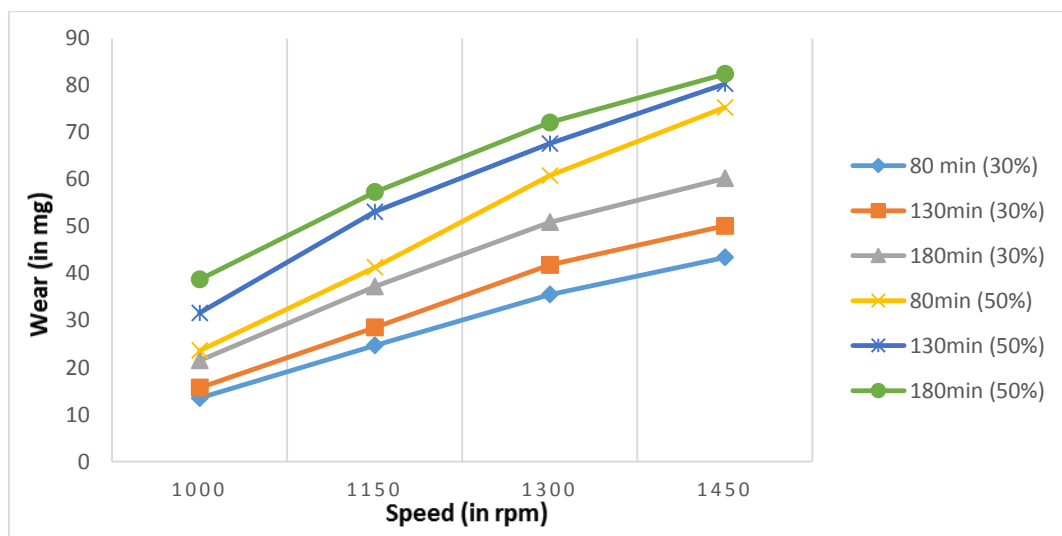


Figure 5.8: Variation of wear (in mg) of Cr₂O₃ coated SS-316 at 30 % and 50 % concentrations

From figures 5.2 and 5.8 it can be noted down that coating has lowered the wear loss in case of SS-316 specimen.

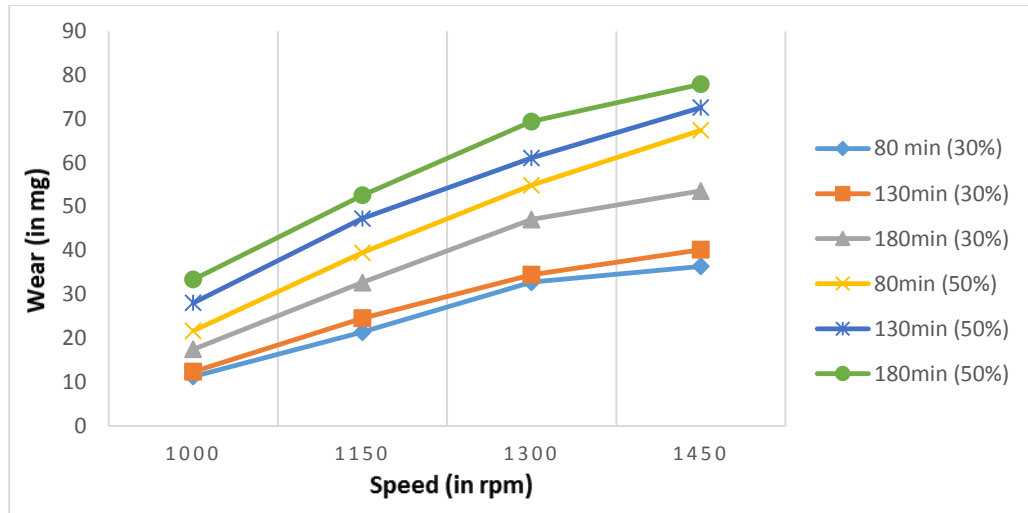


Figure 5.9: Variation of wear (in mg) of Cr₂O₃ coated SS-420 at 30 % and 50 % concentrations

Coating of Cr₂O₃ shows a marginal decrease in wear loss of the material. So SS-420 shows very less wear loss in the coated state than in the uncoated state. Again the trend is the same showing the increase of wear loss with concentration and speed. But it can also be noted that wear loss of WC-17Co coated specimens is less than Cr₂O₃ coated specimens it can be seen by comparing figures 5.4, 5.5, 5.6, 5.7, 5.8 and 5.9. This also justifies the hardness of the materials listed in the previous chapters. Thus from the above figures it can be concluded that with the coating of the material there is a considerable decrease in wear loss and the wear increases with increasing concentrations and speed.

5.1.4 Comparison of erosion wear of uncoated and WC-17Co coated specimens at 30 % concentration

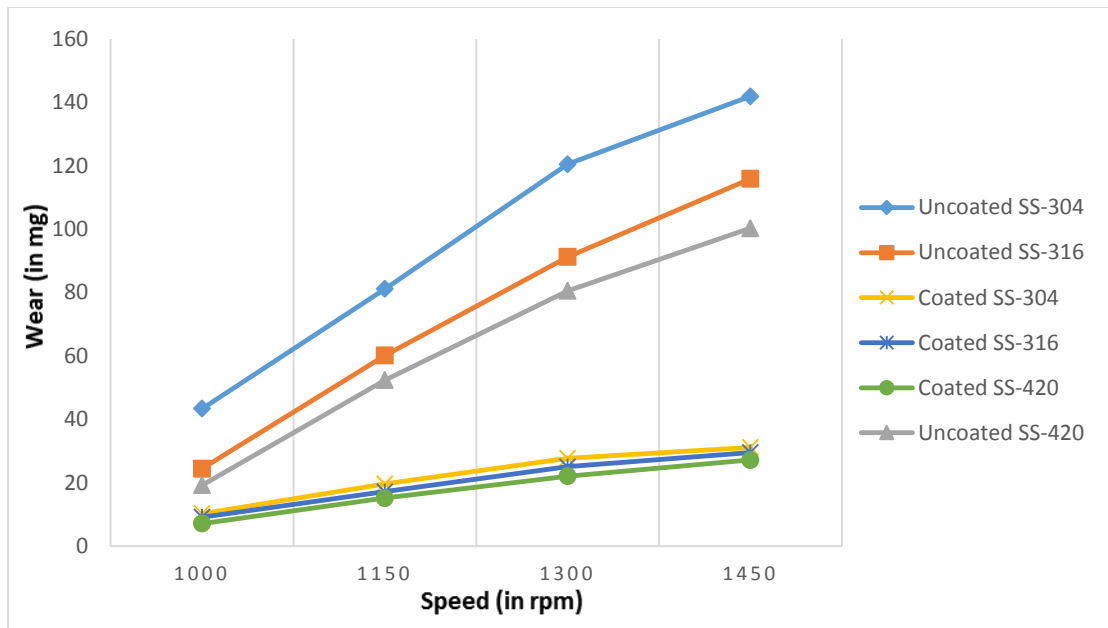


Figure 5.10: Variation of wear (in mg) of uncoated and WC-17Co coated specimens at 80 minutes and 30 % concentration

Figure 5.10 shows the variation of uncoated and WC-17Co coated specimens at 80 minutes and 30 % concentrations. It can be seen from the above graph that the wear loss increases with the speed with the same trend as discussed earlier. This comparison is mainly to compare the wear resistance of coated materials against the uncoated materials. So it is clear from the above graph that there is a huge difference in the material loss of a sample uncoated and the other the coated one.

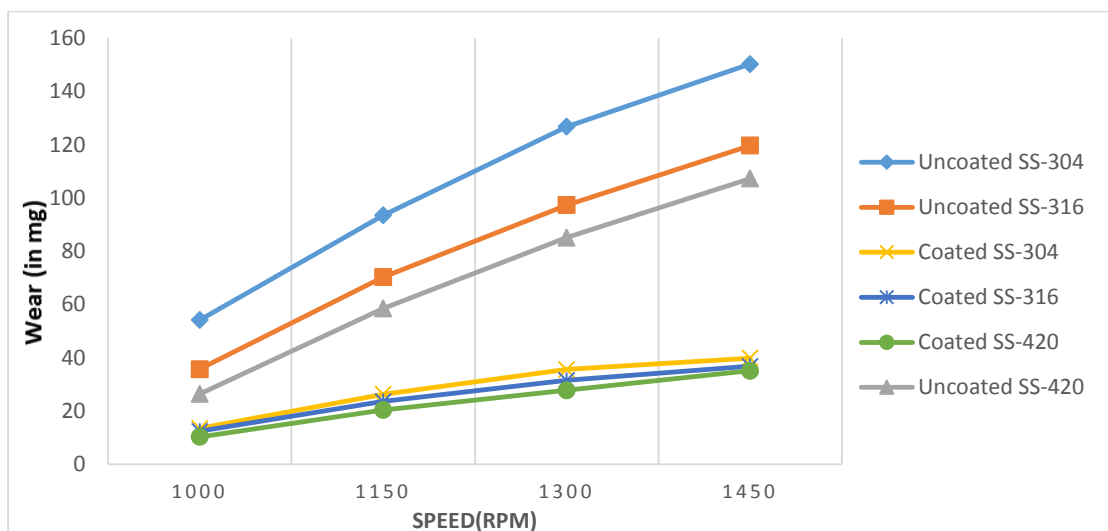


Figure 5.11: Variation of wear (in mg) of uncoated and WC-17Co coated specimens at 130 minutes and 30% concentration

Again there is a huge difference between the wear loss of coated and uncoated samples. But as we compare the figures 5.10 and 5.11, it can be seen that the wear loss has increased in case of 130 minutes. Although the rate of wear is not that large but it has increased. If we compare the difference between the uncoated samples, for instance SS-304 in 80 mins. and 130 mins. , the difference is greater than the wear loss in case of the coated ones.

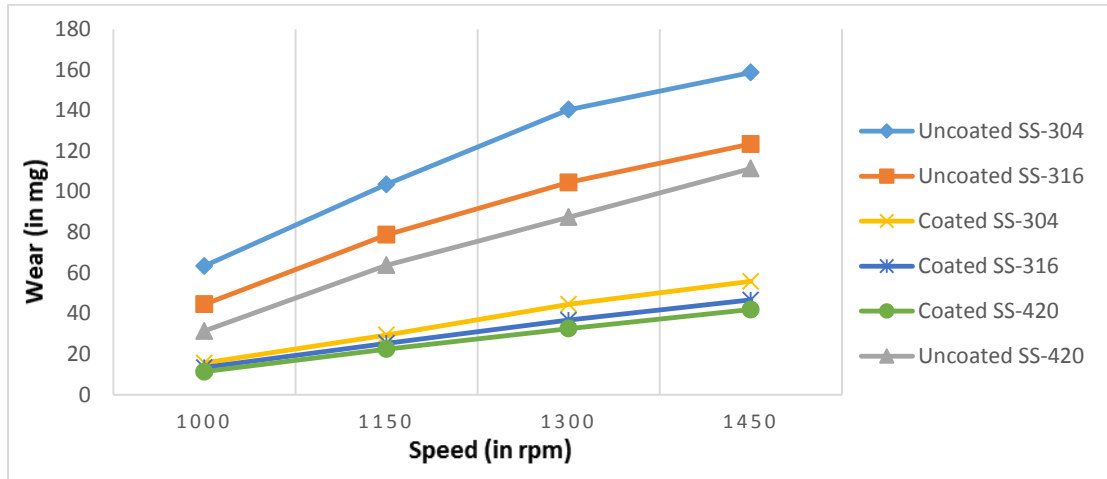


Figure 5.12: Variation of wear (in mg) of uncoated and WC-17Co coated specimens at 180 minutes and 30% concentration

From the figures 5.10, 5.11 and 5.12 it is clear that the wear loss increases with time being greatest for SS-304, SS-316 at the second and SS-420 on the last number. But it is not that dominating parameter as compared to concentration. It can be concluded that the wear loss also depends upon time in a direct manner. Obviously coated specimens show huge erosion resistance as compared to uncoated ones.

5.1.5 Comparison of erosion wear of uncoated and Cr₂O₃ coated specimens at 30 % concentration

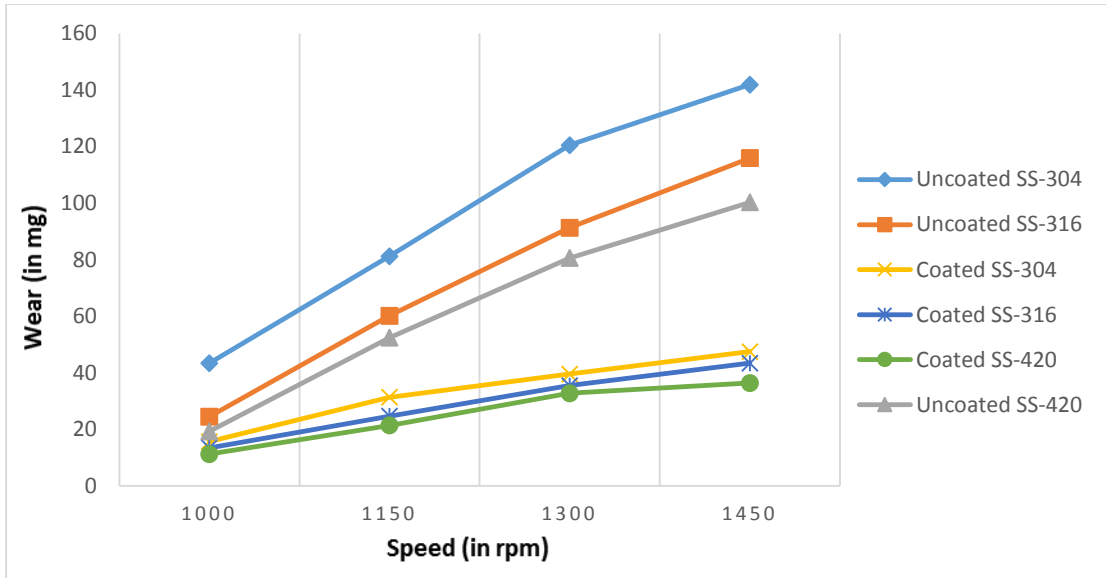


Figure 5.13: Variation of wear (in mg) of uncoated and Cr_2O_3 coated specimens at 80 minutes and 30 % concentration

The above graph shows the variation of wear of uncoated and Cr_2O_3 coated specimens at 80 minutes and 30 % concentration. This also shows the same trend as in the case of WC-17Co. The wear increases with time greatest for uncoated SS-304 and lowest for coated SS-420. But again if we compare the figures 5.10 and 5.13, the wear of coated samples is higher in the Cr_2O_3 coatings but that difference is negligible as there is a huge difference in the wear of uncoated and coated samples.

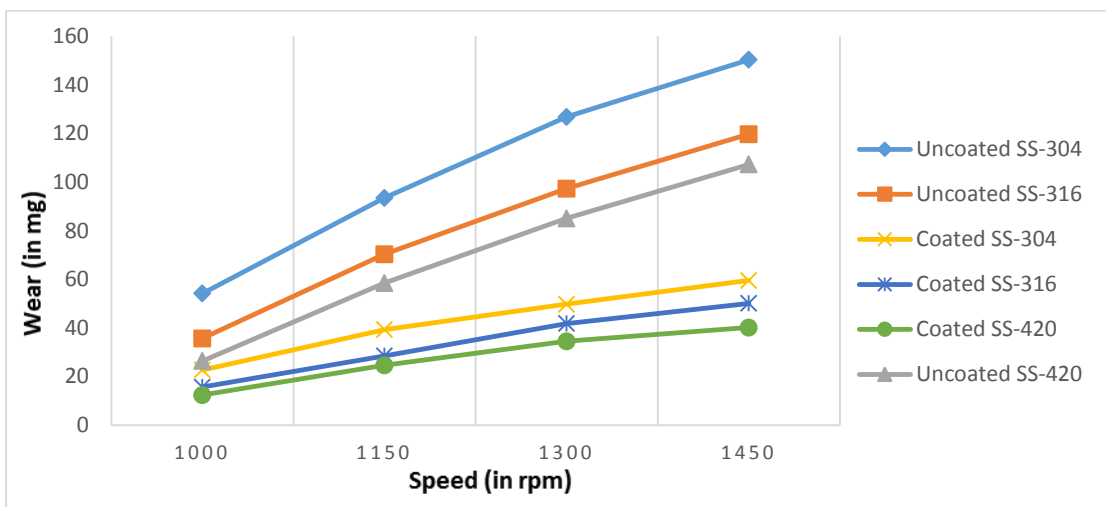


Figure 5.14: Variation of wear (in mg) of uncoated and Cr_2O_3 coated specimens at 130 minutes and 30 % concentration

Figure 5.14 shows the variation of uncoated and Cr_2O_3 coated samples at 30 % concentration and at 130 minutes. The wear has increased as compared to the test conducted at 80 minutes.

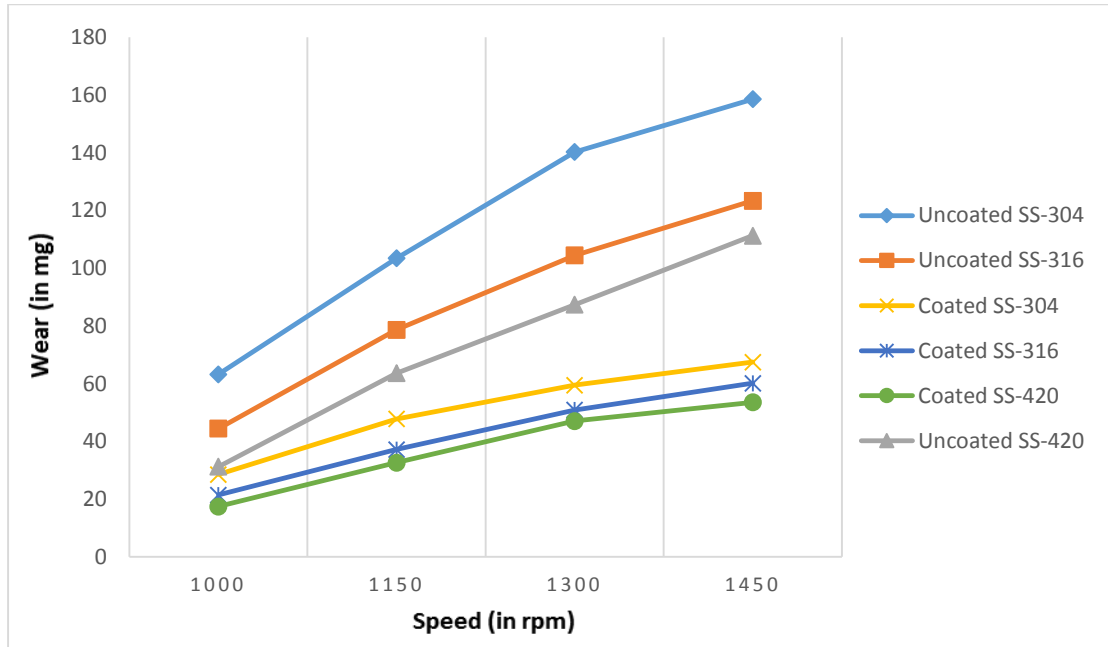


Figure 5.15: Variation of wear (in mg) of uncoated and Cr_2O_3 coated specimens at 180 minutes and 30 % concentration

Comparing figures 5.13, 5.14 and 5.15 it is clear that coating of Cr_2O_3 has increased the resistance to erosion of the base materials. Wear increases with speed and time. Coating of Cr_2O_3 has decreased erosion by almost 2.5 % by weight.

5.1.6 Comparison of erosion wear of uncoated and WC-17Co coated specimens at 50 % concentration

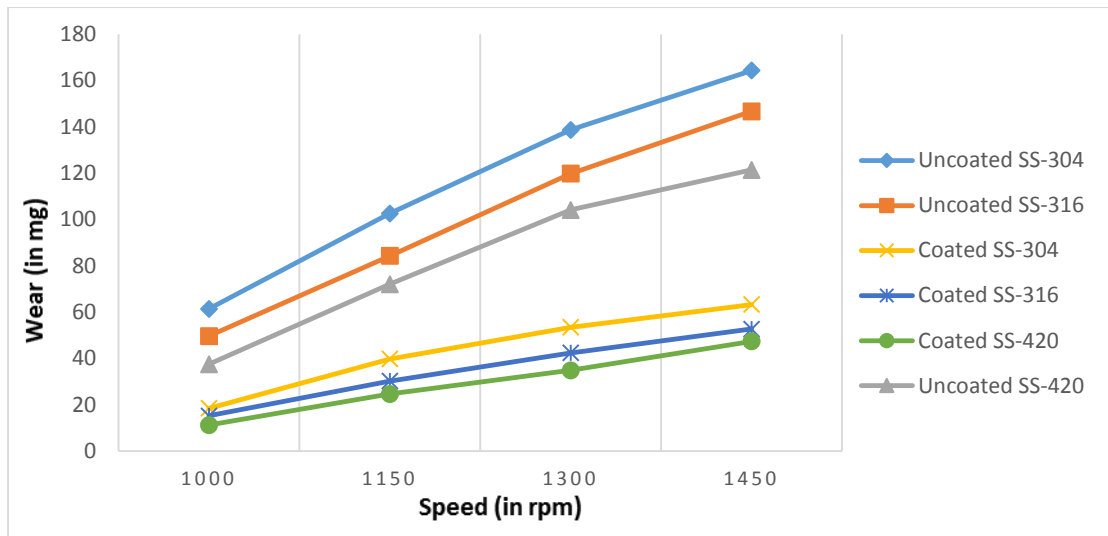


Figure 5.16: Variation of wear (in mg) of uncoated and WC-17Co coated specimens at 80 minutes and 50 % concentration

The above figure shows the erosion wear of uncoated and WC-17Co coated samples at 80 minutes and 50 % concentration. The same tests were conducted at 30 % concentration as shown in figure 5.10. Comparing both the figures, a marginal increase in the wear loss has been observed in the case of 50 % concentration of sand. The other factors like speed, time are also responsible for the wear loss.

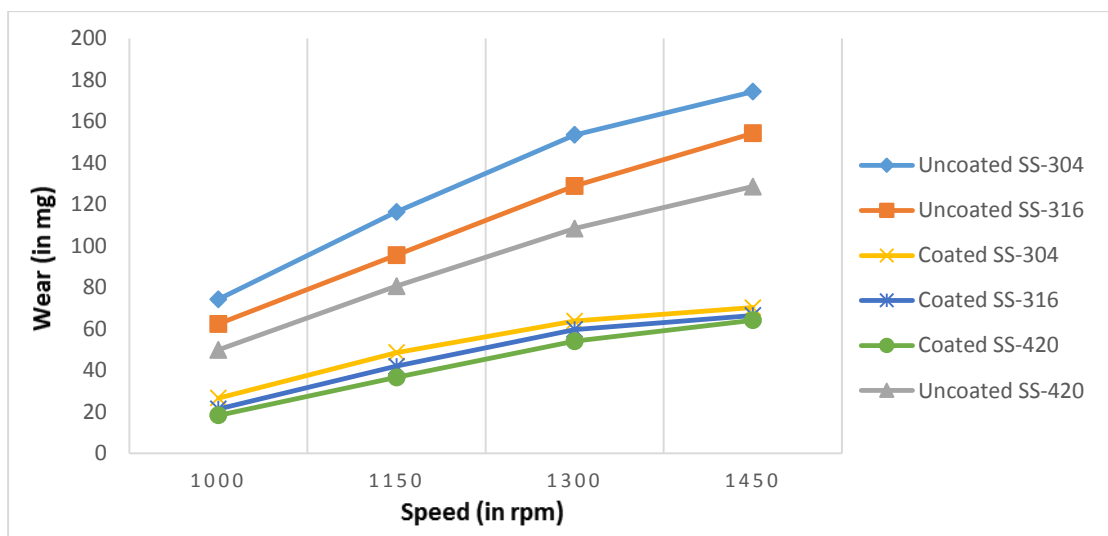


Figure 5.17: Variation of wear (in mg) of uncoated and WC-17Co coated specimens at 130 minutes and 50% concentration

The above figure shows the comparison of wear loss in case of coated and uncoated samples at 130 minutes and 50 % concentration of sand. Comparing it with figure 5.16, it can be observed that with increase in time the wear loss has increased. The coated samples behave quite well against erosion than the uncoated samples. Also comparing with figure 5.11, the concentration increase has also in turn increased the wear loss.

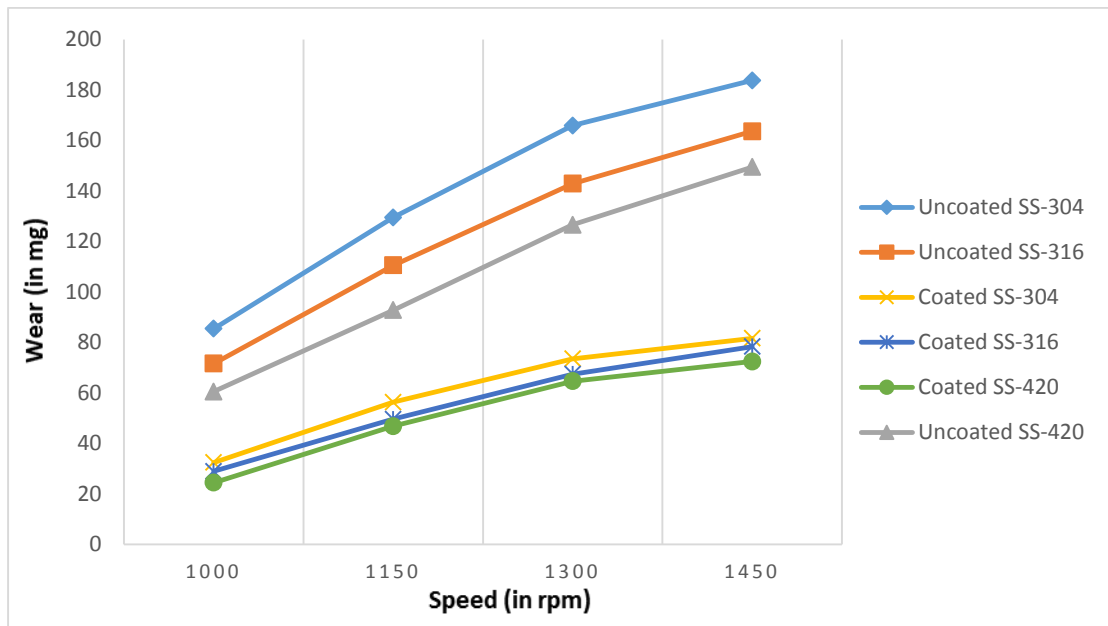


Figure 5.18: Variation of wear (in mg) of uncoated and WC-17Co coated specimens at 180 minutes and 50 % concentration

From the above three figures it can be concluded that the loss of material due to wear increases with time. But concentration is the main factor which dominates the material loss due to erosion. As the results at 50 % were compared with the ones at 30%, it was observed as huge difference in the wear loss being greater in case of 50 % concentration. Other parameters like speed also dominates and follows the same trend as the earlier tests. Coating with WC-Co has decreased the wear loss. Earlier the wear was greatest in uncoated SS-304 and lowest in coated SS-420. This follows the same trend from the very first test conducted due to the difference in hardness of the materials.

5.1.7 Comparison of erosion wear of uncoated and Cr₂O₃ coated specimens at 50% concentration

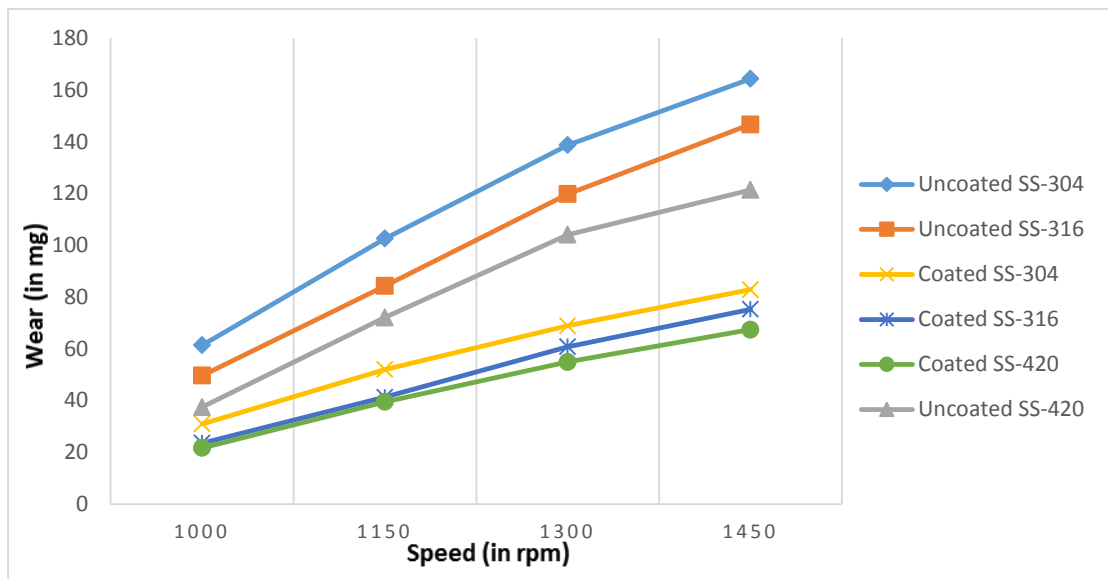


Figure 5.19: Variation of wear (in mg) of uncoated and Cr₂O₃ coated specimens at 80 minutes and 50 % concentration

The above figure shows the results of the tests conducted at 50% concentration at 80 minutes with and without Cr₂O₃ coatings. It shows that the coating has decreased a handsome amount of wear. The wear increases with speed also in case of both coated and uncoated samples. But we compare it with figure 5.16, the erosion performance of coated samples of WC-17Co show less wear loss than Cr₂O₃ coated. Although the difference is very small and is negligible.

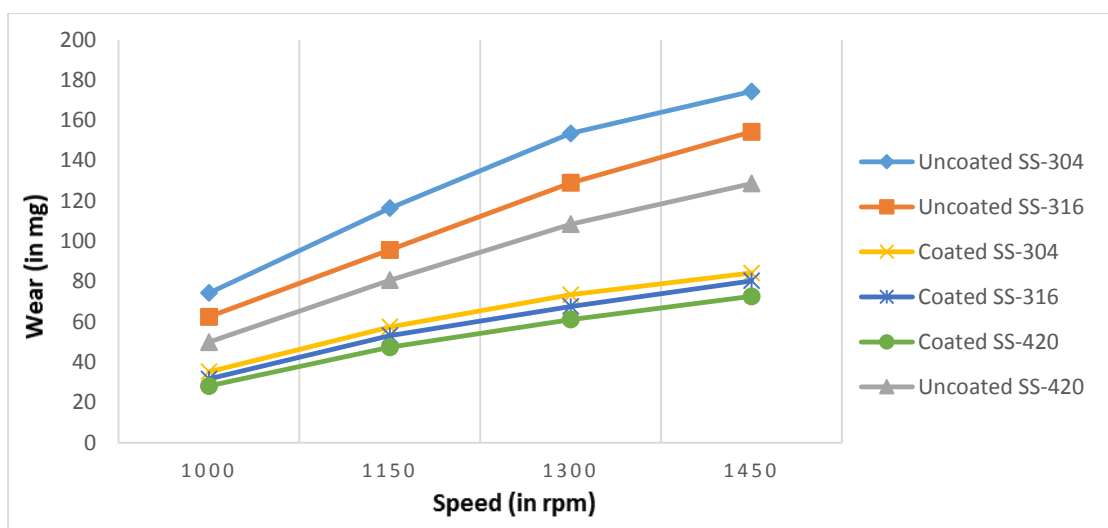


Figure 5.20: Variation of wear (in mg) of uncoated and Cr₂O₃ coated specimens at 130 minutes and 50 % concentration

In the above figure it can be seen that coating has marginally decreased the wear of the samples. The wear loss has increased with the increase in time and speed. Comparing it with figure 5.14 it can be observed that there is greater loss due to wear in case of test conducted at 50 % concentration. So concentration has a great effect on the wear loss of the samples.

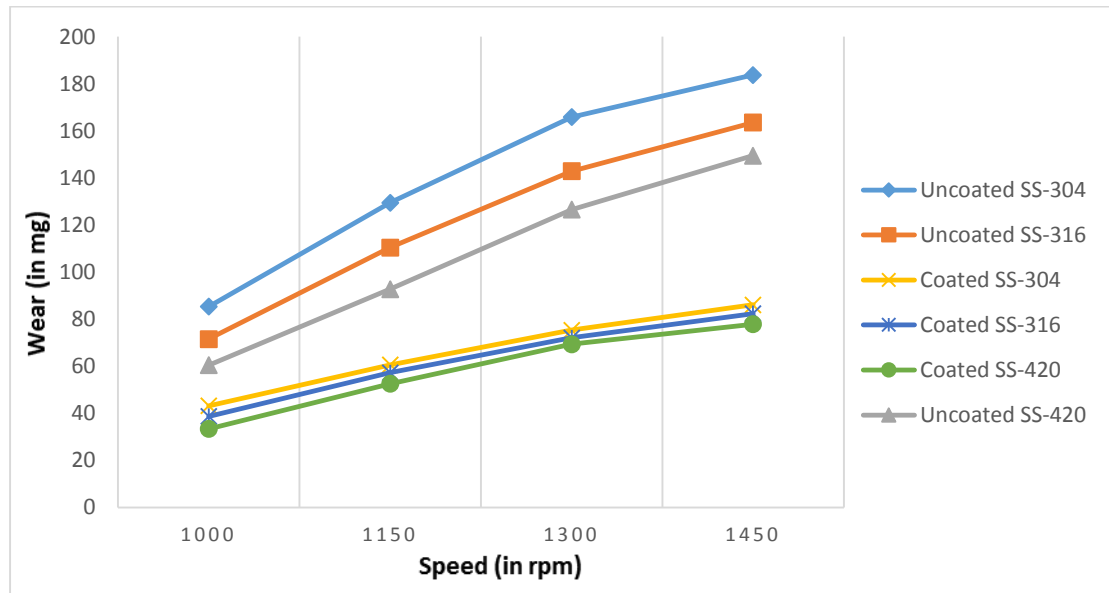


Figure 5.21: Variation of wear (in mg) of uncoated and Cr_2O_3 coated specimens at 180 minutes and 50 % concentration

Studying the above figure shows that the coating of Cr_2O_3 has considerably decreased the amount of wear loss. Comparing figure 5.15 with 5.21, we can see that the wear has increased with increasing concentration of sand in the slurry as both are at same parameters with different concentrations. As we compare it with figures 5.19 and 5.20, it can be observed that with increase in time the wear loss has also increased. Speed also is a big factor in the wear loss of the material. The greatest wear was observed in this case of material SS-304 at 50 % concentration, 180 minutes time and 1450 rpm speed.

5.2 SEM analysis of eroded samples

All the samples were subjected to erosion at 50 % concentration, 130 minutes and at 1450 rpm speed. Following are the images produced by SEM after the erosion wear.

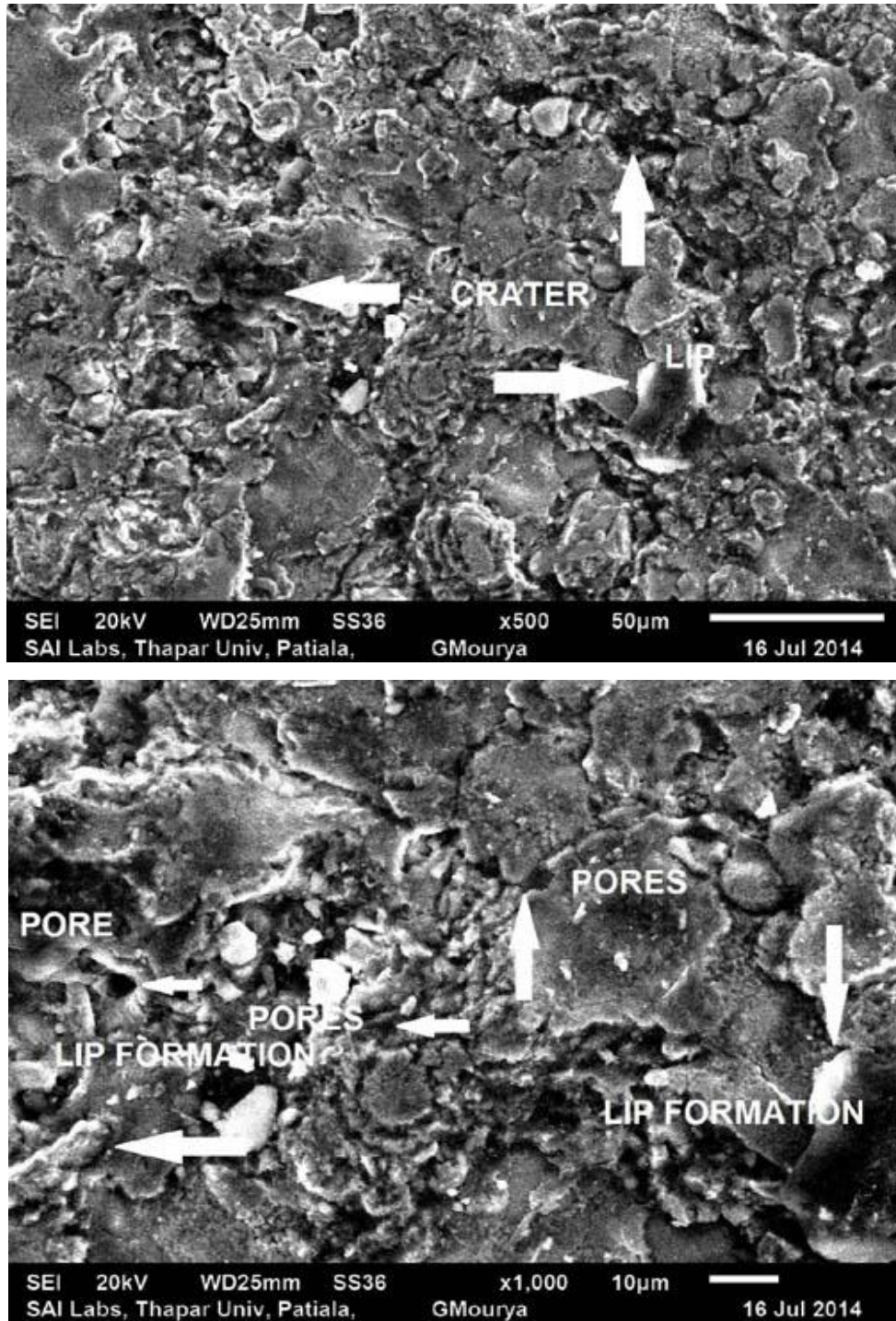


Figure 5.22: SEM analysis of Cr_2O_3 coated SS-304 surface at X500 and X1000

Figure 5.22 shows the images produced by SEM after erosion at 50 % slurry, 130 minutes time and speed at 1450 rpm at magnification of X500 and X1000. The pattern of erosion shows the formation of lips, pores, and craters in the above figure.

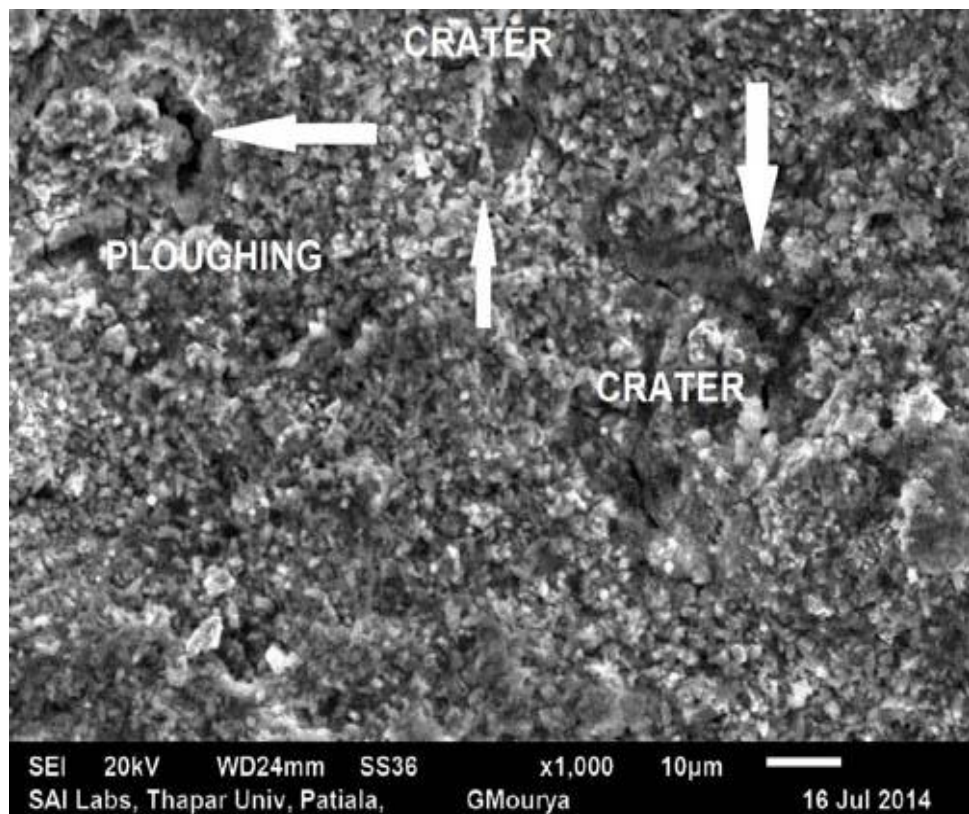
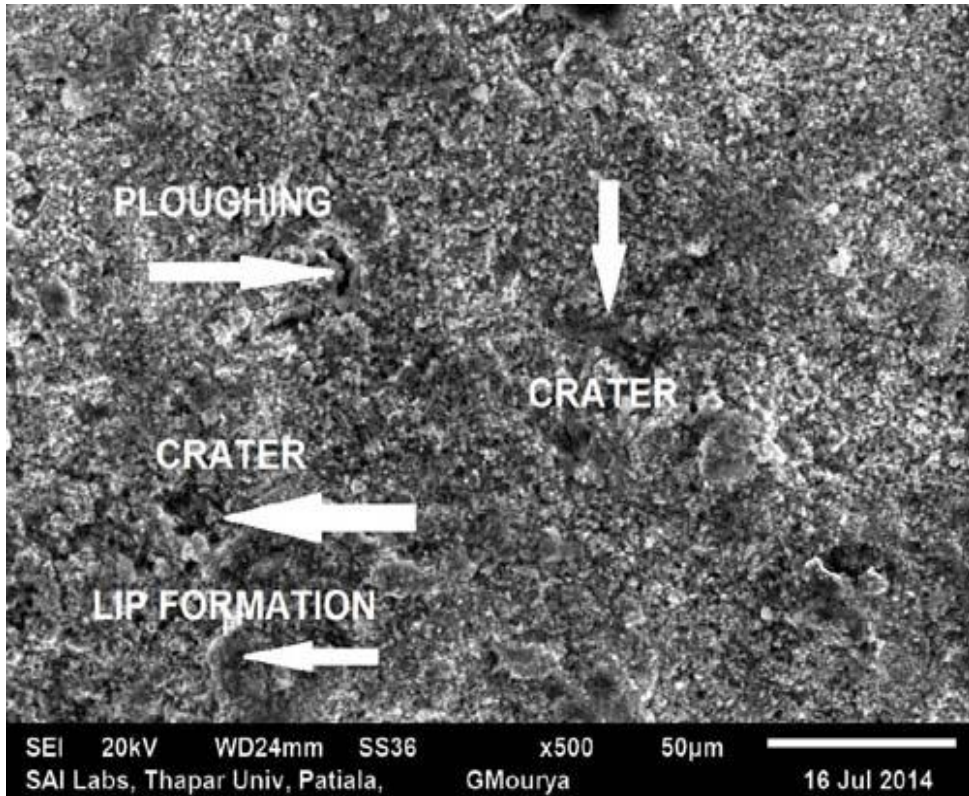


Figure 5.23: SEM analysis of WC-17Co coated SS-304 surface at X500 and X1000

Figure 5.23 shows the SEM analysis of WC-17Co coated SS-304 surface at X500 and X1000 magnification at 50 % slurry, 130 minutes time and speed at 1450 rpm. It shows the patterns of ploughing, lip formation and craters on the surface of the specimen.

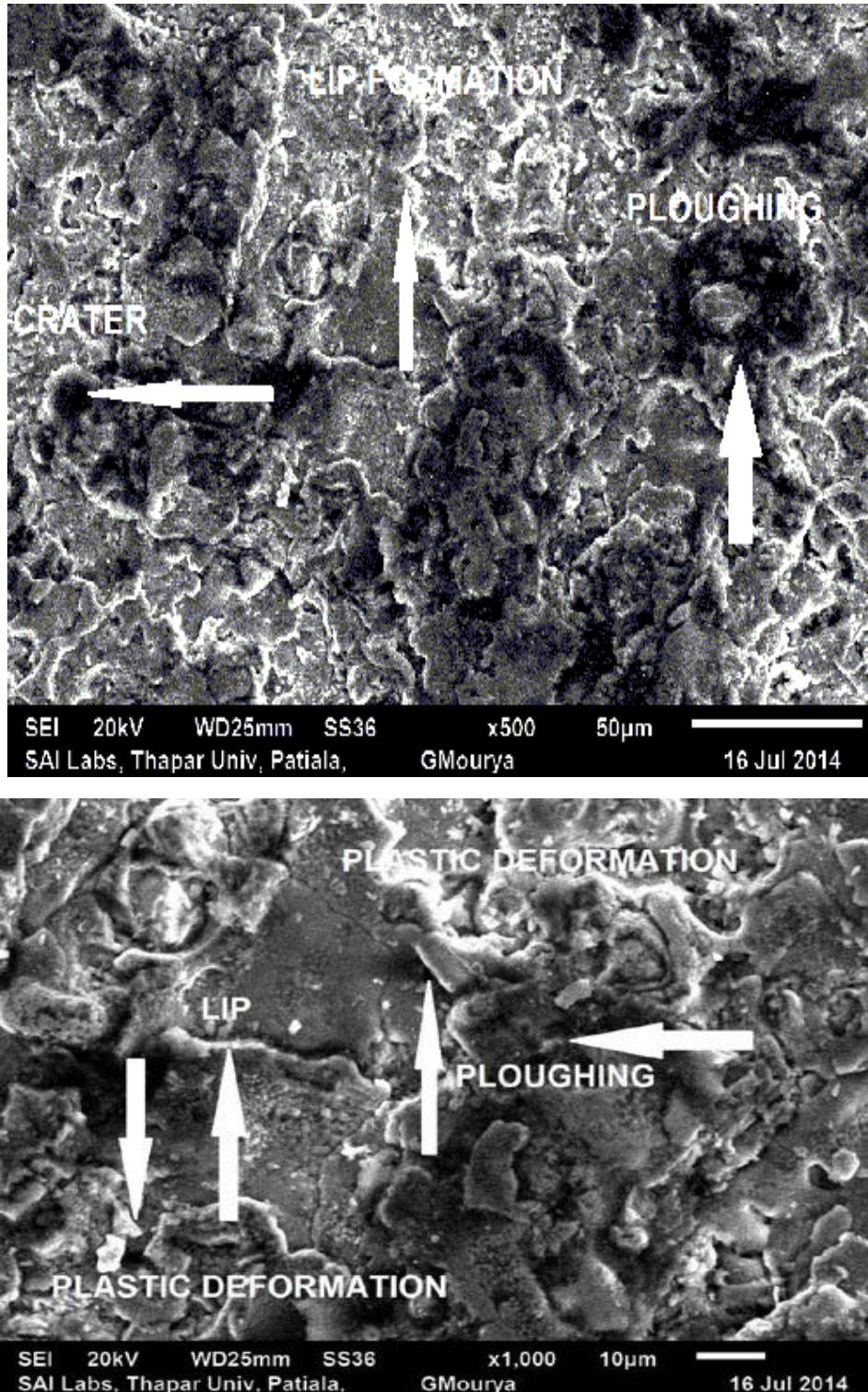


Figure 5.24: SEM analysis of Cr_2O_3 coated SS-316 surface at X500 and X1000

Figure 5.24 shows the SEM analysis of Cr₂O₃ coated SS-316 surface at X500 and X1000 magnification at 50 % slurry, 130 minutes time and speed at 1450 rpm. It shows the patterns of ploughing, lip formation, craters and plastic deformation on the surface of the specimen.

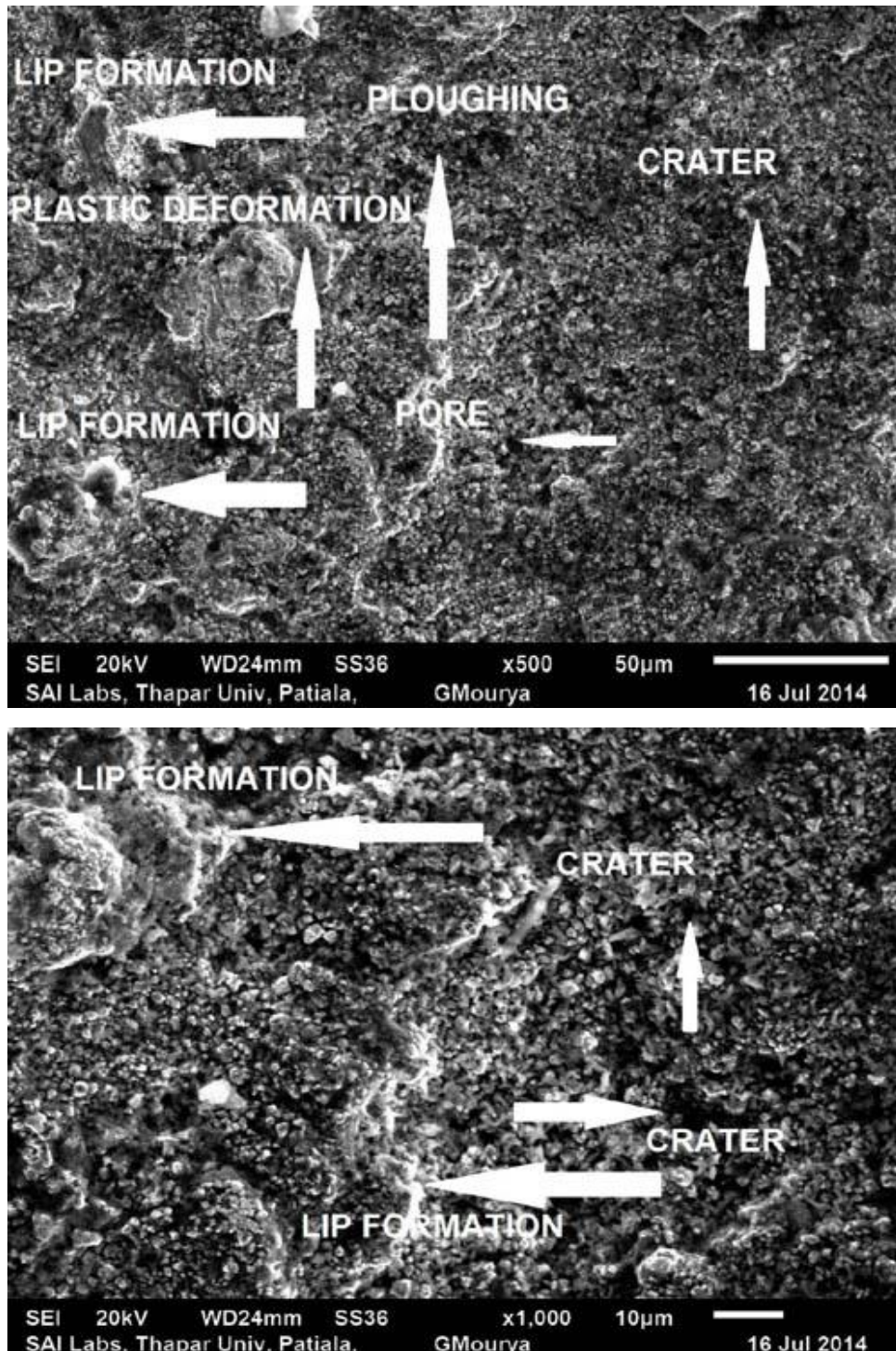


Figure 5.25: SEM analysis of WC-17Co coated SS-316 surface at X500 and X1000

Figure 5.25 shows the SEM analysis of Cr_2O_3 coated SS-316 surface at X500 and X1000 magnification at 50 % slurry, 130 minutes time and speed at 1450 rpm. It shows the patterns of ploughing, lip formation, craters and plastic deformation on the surface of the specimen.

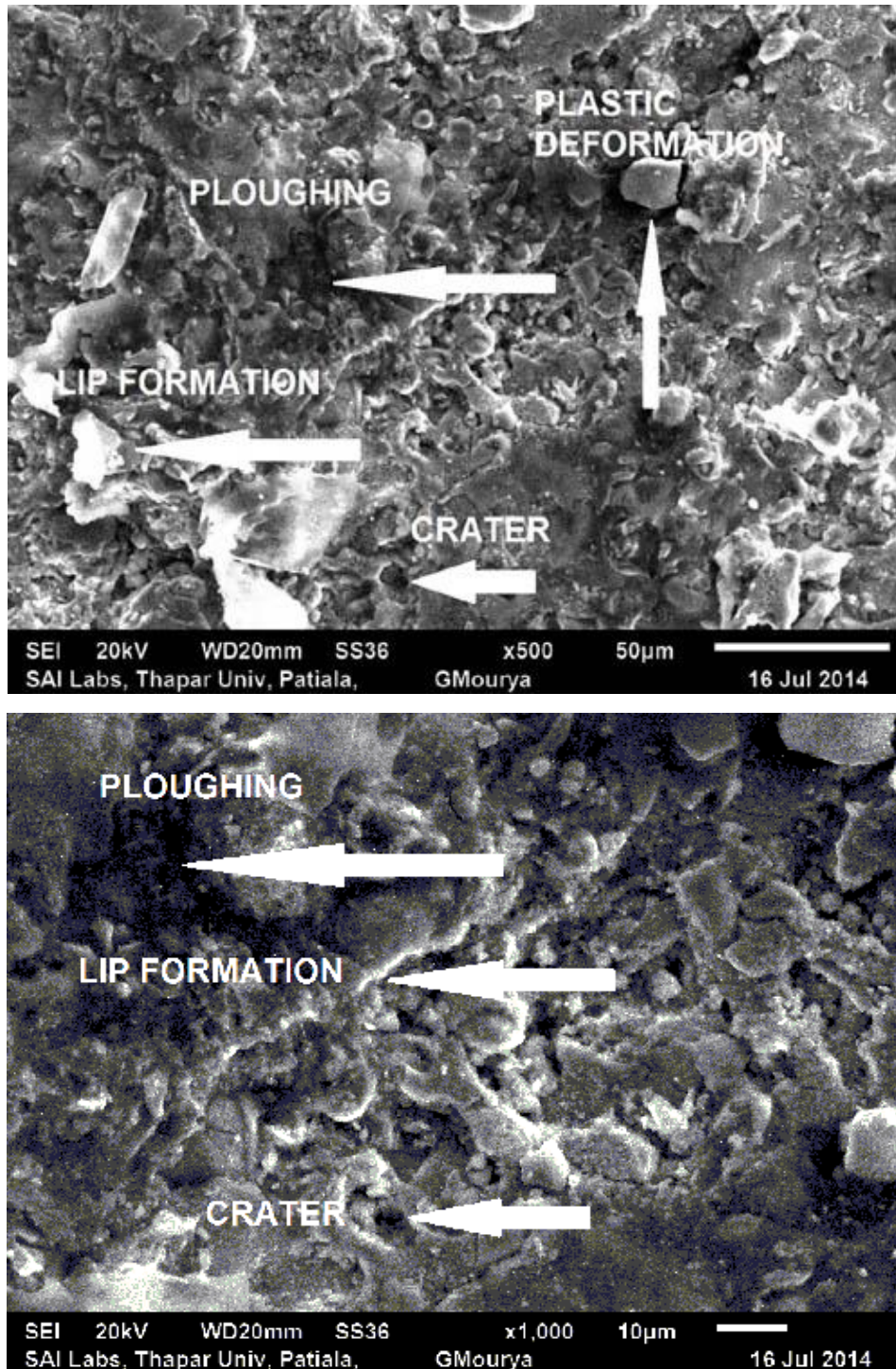


Figure 5.26: SEM analysis of Cr_2O_3 coated SS-420 surface at X500 and X1000

Figure 5.26 shows the SEM analysis of Cr₂O₃ coated SS-420 surface at X500 and X1000 magnification at 50 % slurry, 130 minutes time and speed at 1450 rpm. It shows the patterns of ploughing, lip formation, craters and plastic deformation on the surface of the specimen.

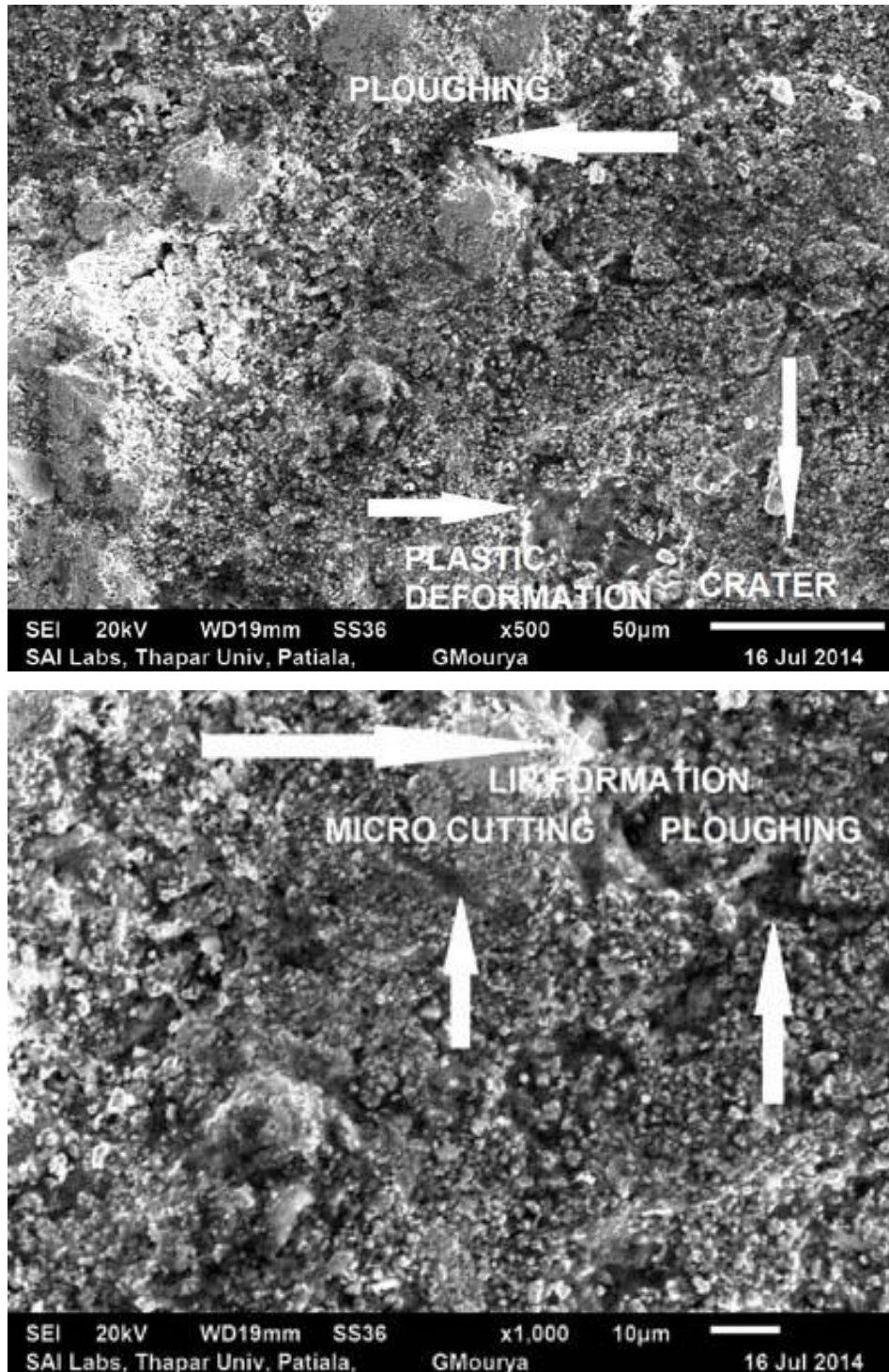


Figure 5.27: SEM analysis of WC-17Co coated SS-420 surface at X500 and X1000

Figure 5.27 shows the SEM analysis of WC-17Co coated SS-420 surface at X500 and X1000 magnification at 50 % slurry, 130 minutes time and speed at 1450 rpm. It shows the patterns of ploughing, lip formation, craters and plastic deformation on the surface of the specimen. A pattern of micro cutting can also be noticed from the above analysis.

Chapter 6

Conclusions

6.1 Conclusions

The erosion wear of turbine steels has been a big problem in hydro power plants all over the world. This problem normally occurs during landslides, heavy rainfalls, floods, etc. The natural processes cannot be controlled by human beings but a material which is most suitable in these conditions can be used for the long life of the turbines. Stainless steels are normally used for the turbines of the power plants. They not only resist erosion wear but also are very safe in corrosive environments. Therefore the stainless steels of grades 304, 316 and 420 were used as base materials in the experiment. To enhance the performance of these materials two types of coatings were used i.e. WC-Co and Cr_2O_3 on these materials. The tests were carried out at two concentrations of sand in water 30 % and 50 %, three time intervals 80 minutes, 130 minutes and 180 minutes, four speeds 1000 rpm, 1150 rpm, 1300 rpm and 1450 rpm. The followings are the conclusions from the results that are discussed in the last chapter.

- The erosion of purely base material at different parameters show uniform wear
- Concentration of sand in water is found out to be the major dominating factor in the erosion wear.
- The erosion wear increased rapidly with increasing concentrations of sand in water.
- Other major factor is speed which also increases the erosion wear.
- Time is also a factor which contributes to erosion but is not that dominating.
- Erosion wear of the coated samples showed great resistance to erosion wear.
- The WC-Co coated samples showed better erosion resistance upto 3.5 times that of base material.
- The Cr_2O_3 coated samples showed improvement in erosion resistance upto 2.7 times as compared to the uncoated samples.
- So due to coatings the wear loss has decreased to a great amount.
- The erosion wear at speed of 1450 rpm was always highest in all the tests.
- The samples showed better erosion resistance at 30% concentration of sand than at 50%.

6.2 Future scope

- Materials other than stainless steels can be used for analysing the performance of erosion wear.
- The same tests and their analysis can also be carried out by other computational techniques on the software like ANSYS.
- Coatings of other hard materials can be used for the erosion wear tests.
- Different testing rigs can be used for same parameters.
- Parameters of different values can also be used to compare the performance of the materials in erosive environment.

References

- [1] J.P. Tu, L.P. Zhu, H.X. Zhao, Slurry erosion characteristics of TiN coatings on α -Ti and plasma-nitrided Ti alloy substrates, *Surface and Coatings Technology* 122, 1999, pp. 176-182.
- [2] D.W. Wheeler, R.J.K. Wood, Erosion of hard surface coatings for use in offshore gate valves, *Wear* 258, 2005, pp. 526-536.
- [3] V.A.D. Souza, A. Neville, Corrosion and synergy in a WC Co Cr HVOF thermal spray coating - understanding their role in erosion - corrosion degradation, *Wear* 259, 2005, pp. 171-180.
- [4] B.S. Mann, Vivek Arya, A.K. Maiti, M.U.B. Rao, Pankaj Joshi, Corrosion and erosion performance of HVOF/TiAlN PVD coatings and candidate materials for high pressure gate valve application, *Wear* 260, 2006, pp. 75-82.
- [5] A.K. Maiti, N. Mukhopadhyay, R. Raman, Effect of adding WC powder to the feedstock of WC-Co-Cr based HVOF coating and its impact on erosion and abrasion resistance, *Surface & Coatings Technology* 201, 2007, pp. 7781-7788.
- [6] Hazoor Singh Sidhu, Buta Singh Sidhu, S. Prakash, Solid particle erosion of HVOF sprayed NiCr and Stellite-6 coatings, *Surface & Coatings Technology* 202, 2007, pp. 232-238.
- [7] J.F. Santa, J.C. Baena, A. Toro, Slurry erosion of thermal spray coatings and stainless steels for hydraulic machinery, *Wear* 263, 2007, pp. 258-264.
- [8] T. Manisekaran, M. Kamaraj, S.M. Sharrif, and S.V. Joshi, Slurry Erosion Studies on Surface Modified 13Cr-4Ni Steels: Effect of Angle of Impingement and Particle Size, *Journal of Materials Engineering and Performance* 16, 2007, pp. 567-572.
- [9] J.F. Santa, L.A. Espitia, J.A. Blanco, S.A. Romo, A. Toro, Slurry and cavitation erosion resistance of thermal spray coatings, *Wear* 267, 2009, pp. 160-167.
- [10] Girish R. Desale, Bhupendra K. Gandhi, S.C. Jain, Particle size effects on the slurry erosion of aluminium alloy (AA 6063), *Wear* 266, 2009, pp. 1066-1071.
- [11] M.K. Padhy, R.P. Saini, Effect of size and concentration of silt particles on erosion of Pelton turbine buckets, *Energy* 34, 2009, pp. 1477-1483.
- [12] Zhou Guanghong, Ding Hongyan, ZhangYue, Li Nianlian, Corrosion-erosion wear behaviors of 13Cr24Mn0.44N stainless steel in saline-sand slurry, *Tribology International* 43, 2010, pp. 891-896.

- [13] C.W. Lee, J.H. Han, J. Yoon, M.C. Shin, S.I. Kwun, A study on powder mixing for high fracture toughness and wear resistance of WC-Co-Cr coatings sprayed by HVOF, *Surface & Coatings Technology* 204, 2010, pp. 2223-2229.
- [14] S.L. Liu, X.P. Zheng, G.Q. Geng, Influence of nano-WC-12Co powder addition in WC-10Co-4Cr AC-HVAF sprayed coatings on wear and erosion behaviour, *Wear* 269, 2010, pp. 362-367.
- [15] C.S. Ramesh, D.S. Devaraj, R. Keshavamurthy, B.R. Sridhar, Slurry erosive wear behaviour of thermally sprayed Inconel-718 coatings by APS process, *Wear* 271, 2011, pp. 1365-1371.
- [16] S.L. Jiang, H.X. Hu, Y.S. Tao, T.Y. Xiong, Y.G. Zheng, Cavitation erosion and jet impingement erosion mechanism of cold sprayed Ni-Al₂O₃ coating, *Nuclear Engineering and Design* 241, 2011, pp. 4929-4937.
- [17] Lalit Thakur, N. Arora, R. Jayaganthan, R. Sood, An investigation on erosion behavior of HVOF sprayed WC-CoCr coatings, *Applied Surface Science* 258, 2011, pp. 1225-1234.
- [18] Raghuvir Singh, S.K. Tiwari, Suman K. Mishra, Cavitation Erosion in Hydraulic Turbine Components and Mitigation by Coatings: Current Status and Future Needs, *Journal of Materials Engineering and Performance* 21, 2011, pp. 1539-1551.
- [19] S.S. Rajahram, T.J. Harvey, R.J.K. Wood, Electrochemical investigation of erosion-corrosion using a slurry pot erosion tester, *Tribology International* 44, 2011, pp. 232-240.
- [20] Vinay Pratap Singh, Anjan Sil, R. Jayaganthan, Tribological behavior of plasma sprayed Cr₂O₃-3%TiO₂ coatings, *Wear* 272, 2011 pp. 149-158.
- [21] Y. Yang, Y.F. Cheng, Parametric effects on the erosion–corrosion rate and mechanism of carbon steel pipes in oil sands slurry, *Wear* 276-277, 2012, pp. 141-148.
- [22] J.A. Alegria-Ortega, L.M. Ocampo-Carmona, F.A. Suarez-Bustamante, J.J. Olaya-Florez, Erosion–corrosion wear of Cr/CrN multi-layer coating deposited on AISI-304 stainless steel using the unbalanced magnetron (UBM) sputtering system, *Wear* 290-291, 2012, pp. 149-153.
- [23] Deepak Kumar Goyal, Harpreet Singh, Harmesh Kumar, Varinder Sahni, Slurry erosion behaviour of HVOF sprayed WC–10Co–4Cr and Al₂O₃+13TiO₂ coatings on a turbine steel, 2012, *Wear* 289, pp. 46-57.
- [24] H.J. Amarendra, G.P. Chaudhari, S.K. Nath, Synergy of cavitation and slurry erosion in the slurry pot tester, *Wear* 290-291, 2012, pp. 25-31.

- [25] S.A. Romo, J.F. Santa, J.E. Giraldo, A. Toro, Cavitation and high-velocity slurry erosion resistance of welded Stellite 6 alloy, *Tribology International* 47, 2012, pp. 16-24.
- [26] B. Rajkarnikar, H.P. Neopane, B.S. Thapa, Development of rotating disc apparatus for test of sediment-induced erosion in Francis runner blades, *Wear* 306, 2013, pp. 119-125.
- [27] H.S. Arora, H.S. Grewal, H. Singh, S. Mukherjee, Zirconium based bulk metallic glass - Better resistance to slurry erosion compared to hydro turbine steel, *Wear* 307, 2013, pp. 28-34.
- [28] H.S. Grewal, H.S. Arora, H. Singh, A. Agrawal, Surface modification of hydroturbine steel using friction stir processing, *Applied Surface Science* 268, 2013, pp. 547-555.
- [29] Sheng Hong, Yuping Wu, Qian Wang, Guobing Ying, Gaiye Li, Wenwen Gao, Bo Wang, Wenmin Guo, Microstructure and cavitation-silt erosion behavior of high-velocity oxygen-fuel (HVOF) sprayed Cr_3C_2 -NiCr coating, *Surface & Coatings Technology* 225, 2013, pp. 85-91.
- [30] Xiulin Ji, Jianhua Zhao, Xunwei Zhang, Meiying Zhou, Erosion-corrosion behavior of Zr-based bulk metallic glass in saline-sand slurry, *Tribology International* 60, 2013, pp. 19-24.
- [31] Feng Cheng, Shuyun Jiang, Cavitation erosion resistance of diamond-like carbon coating on stainless steel", *Applied Surface Science* 292, 2014, pp. 16-26.